Journal of Marine Research, 61, 659–691, 2003

Form, performance and trade-offs in swimming and stability of armed larvae

by Daniel Grünbaum[1] and Richard R. Strathmann[2,3]

ABSTRACT

Diverse larval forms swim and feed with ciliary bands on arms or analogous structures. Armed morphologies are varied: numbers, lengths, and orientations of arms differ among species, change through development, and can be plastic in response to physiological or environmental conditions. A hydromechanical model of idealized equal-armed larvae was used to examine functional consequences of these varied arm arrangements for larval swimming performance. With effects of overall size, ciliary tip speed, and viscosity factored out, the model suggested trade-offs between morphological traits conferring high swimming speed and weight-carrying ability in still water (generally few arms and low arm elevations), and morphologies conferring high stability to external disturbances such as shear flows (generally many arms and high arm elevations). In vertical shear, larvae that were passively stabilized by a center of buoyancy anterior to the center of gravity tilted toward and consequently swam into downwelling flows. Thus, paradoxically, upward swimming by passively stable swimmers in vertical shear resulted in enhanced downward transport. This shear-dependent vertical transport could affect diverse passively stable swimmers, not just armed larvae. Published descriptions of larvae and metamorphosis of 13 ophiuroids suggest that most ophioplutei fall into two groups: those approximating modeled forms with two arms at low elevations, predicted to enhance speed and weight capacity, and those approximating modeled forms with more numerous arms of equal length at high elevations, predicted to enhance stability in shear.

1. Introduction

Diverse planktonic larval forms swim and feed with bands of cilia. In many of these forms, ciliary bands are extended on arms, tentacles, or lobes. These extensions occur in echinoderm plutei, inarticulate brachiopod larvae, phoronid actinotrochs, actinula larvae of trachyline medusae, and some gastropod veligers. Maximum rates of clearing food particles from suspension depend on lengths of the ciliary bands that capture particles (Strathmann, 1971; Hart, 1996), and one way to increase lengths of ciliary bands and clearance rates is to deploy the bands on long extensions of the larval body. High clearance rates are useful when food is scarce, and plutei develop longer arms when growing with

1. School of Oceanography, University of Washington, Seattle, Washington, 98195-7940, U.S.A. ***email: grunbaum@ocean.washington.edu***

2. Friday Harbor Marine Laboratories, University of Washington, 620 University Road, Friday Harbor, Washington, 98250, U.S.A.

3. Department of Biology, University of Washington, Seattle, Washington, 98195-1800, U.S.A.

scarcer food (Boidron-Metairon, 1988; Strathmann *et al.,* 1992; Hart and Strathmann, 1994).

These ciliated extensions of the body are effective in feeding, but there are several indications that they are not especially effective in swimming. Evolutionary loss of the need for food is associated with loss of arms in larvae that continue to swim (Strathmann, 1975; Emlet, 1991, 1994; Wray, 1995). This suggests that for swimming, cilia are more effectively deployed in transverse rings or broad fields. Body extensions can compromise swimming several ways. Long body dimensions are exposed to greater shear and passive drag (Emlet, 1983). Anterior arms of plutei are associated with a posterior counterweight for a stable orientation, and the counterweight increases larval density and sinking rates (Pennington and Strathmann, 1990). These observations suggest that extension of ciliary bands on arms or tentacles enhances feeding but compromises swimming.

This study examines relationships between larval swimming performance and geometry of arms and centers of gravity and buoyancy, and investigates how well pluteus-like larvae meet design criteria for performance in swimming. The modeled larvae are pluteus-like, in that the arms are thin, straight, and rigid, and provide propulsion through lateral ciliary bands (Figs. 1 and 2). A morphospace is explored that includes variation in number, length, angle, and spacing of arms, plus distributions of density that affect passive gravitational stability. The design criteria concern swimming and sinking speeds, capacity to carry a load, and stability in shear flows. Many larvae swim upward or migrate vertically (Pennington and Emlet, 1986; Young, 1995; Forward and Tankersley, 2001). Speed and stability both affect a larva's ability to change its position in the water column. Shear can reorient swimming larvae, changing the direction of swimming away from the vertical or other preferred orientation. Arm geometry and distribution of density within the larval body affect rotation in shear. Relatively dense objects carried by larvae include their skeletons and rudiments of developing juvenile structures. These and other dense structures are often positioned posteriorly, conferring passive vertical orientation.

This paper addresses the question, how is evolution of larval forms functionally constrained by the hydromechanical consequences of alternative morphologies? The objective is to establish some basic principles concerning how body extensions that are effective in feeding affect performance in swimming, and to test hypotheses about functional morphology in pluteus-like larvae:

1. Requirements for swimming speed, weight-bearing capacity, and passive sinking speed functionally constrain the number, length and position of larval arms.

2. Requirements for hydrodynamic stability functionally constrain the number, length and position of larval arms.

Hypothesis 1 implies that alternative larval arm geometries differ in performance, and that larval arms are constitutively or facultatively positioned in postures favorable for high swimming rates, high weight-bearing capacities, and low passive sinking speeds. Similarly, Hypothesis 2 implies that alternative morphologies differ in their stability to flow

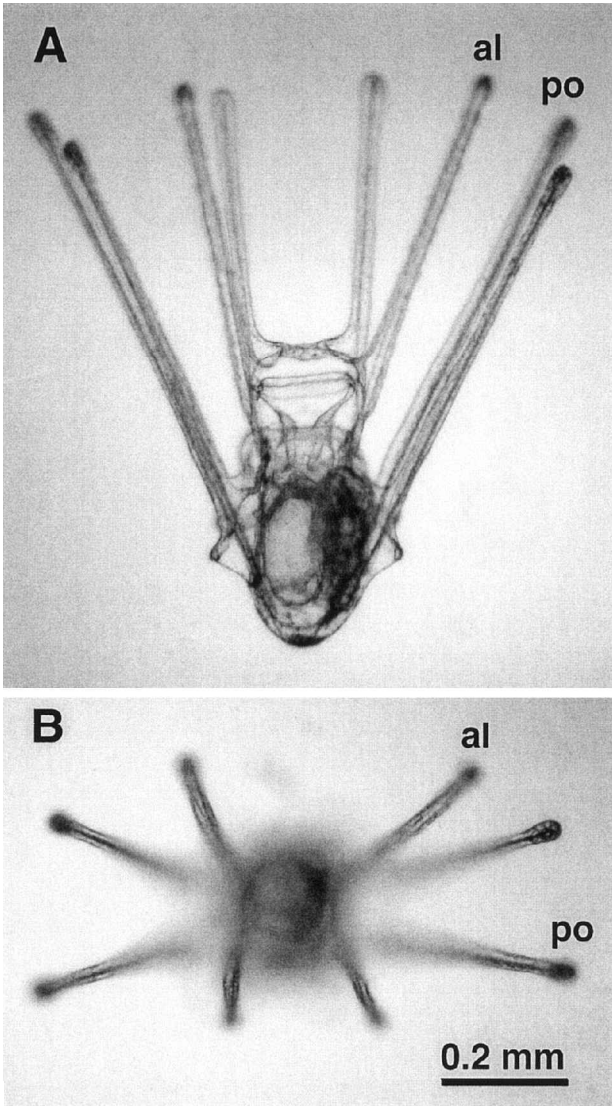

Figure 1. Two views of a pluteus of the sand dollar, *Dendraster excentricus* at the 8-arm stage. Labels indicate postoral arms (po) and anterolateral arms (al).

disturbances such as shear and turbulence, and that existing larval forms adopt favorable arm postures for maintaining stable orientations. A further hypothesis is

3. Morphologies favorable for maximizing swimming speeds and weight capacities and for minimizing sinking speeds differ from those maximizing stability.

Hypothesis 3 implies that there are evolutionary trade-offs between various aspects of swimming performance, and that existing pluteus-like larval forms will reflect compromise

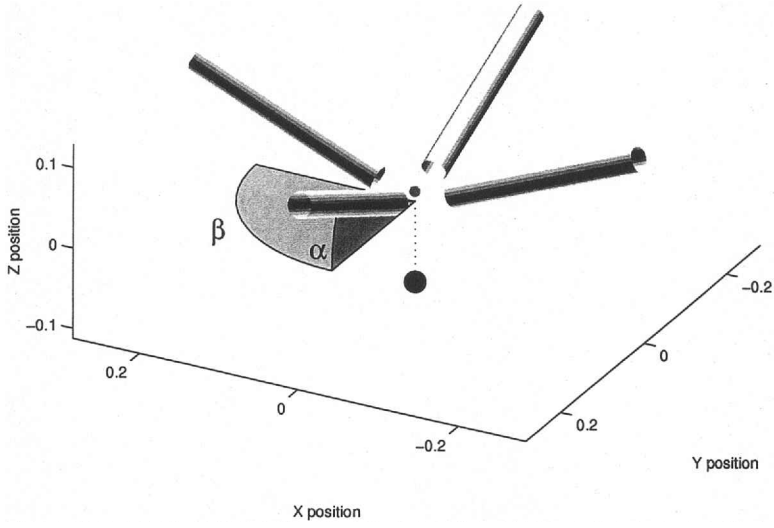

Figure 2. Larval morphology is defined in the model by the number, size and orientation of the arms, and by the centers of buoyancy and gravity ($\mathbf{X}_{buoy}$ and $\mathbf{X}_{grav}$) and their associated forces ($\mathbf{F}_{buoy}$ and $\mathbf{F}_{grav}$). The elevation angle of each arm above the XY plane is α, and the rotation angle of each arm about the Z axis from the X axis is β. The position of $\mathbf{X}_{buoy}$ is indicated by a small gray sphere, which in this case is coincident with the reference position for the larva, located at the origin ($\mathbf{X}_L$). $\mathbf{X}_{grav}$ is indicated by a larger black sphere posterior to $\mathbf{X}_{buoy}$, in a position that confers passive stability. Lateral ciliary bands on each arm are modeled as a tangential velocity perpendicular to the axis of the arm. The strength of this velocity varies with the cosine of the angle off the plane containing the band, illustrated here with dark shading representing higher velocities and lighter shading representing lower velocities (see text and Grünbaum, 1998, for details). Arm geometry is additionally specified by the distances of the arm endpoints relative to the origin (R_{min} and R_{max}) and by arm diameter, D_{arm}.

morphologies that balance opposing requirements. It is reasonable to expect the relative importance of these swimming performance measures to differ across taxa, across stages within taxa, and between phenotypically different individuals of the same species and stage. Hypotheses 1–3 suggest that design criteria of the type investigated in this paper may underlie and help explain some of the morphological and behavioral variations among these types of individuals.

The hypotheses are addressed by developing an idealized model of larval swimming. The model assumes that larvae are small and slow-moving, and that therefore simplifying assumptions can be made about their hydrodynamic interactions with the surrounding seawater. These interactions are determined in part by the Reynolds number, $\mathcal{R}e = (LV\rho/\mu)$, where L and V are characteristic length and speed scales of the larva, μ is the viscosity and ρ is the density. $\mathcal{R}e$ is an index of the relative importance of inertial and viscous effects on flow (Batchelor, 1983). The model assumes that $\mathcal{R}e$ for the larva is sufficiently small that inertial effects on fluid motions can be neglected. Given these

assumptions, the model calculates larval movements by balancing viscous and pressure forces in the fluid and fluid interactions with the larva's ciliated and unciliated surfaces.

This study is restricted to larvae or parts of larvae that can be modeled as arrays of slender cylinders. This makes it possible to use solution techniques from fluid dynamics to solve flows that would be much more difficult with other methods. Attention is restricted here to larval morphologies in which arms are equal and the centers of gravity and buoyancy are along the central axis (as in Fig. 2). Alternative morphologies are discussed elsewhere (Grünbaum and Strathmann, in prep.). The modeled morphologies fit no existing larval forms exactly. However, they fit a great many larval forms approximately. By adopting this simplified morphological approximation, this study attempts to identify some of the unifying general design criteria common to diverse taxa, and to provide a context for more insightful comparative studies of larval functional morphology.

2. Model description

This section presents a partial description of our model in terms accessible to a general biological audience. Additional description for readers interested in technical details are in the Appendix and references cited there.

In the model, the geometry of each larval arm is specified by its elevation angle, α, and rotation angle, β, with respect to the reference point X_L; by the arm's diameter, D_{arm}; and by the radii demarcating the base and tip of the arm, R_{min} and R_{max} (Fig. 2). Each arm is modeled as being composed of a set of slender cylindrical segments. Our model is based on *slender body theory,* an approximation technique that allows us to analytically estimate the velocity distribution around slender cylindrical elements embedded in a flow, and the resulting forces exerted by the fluid on those elements (Hancock, 1953; Blake and Chwang, 1974; Chwang and Wu, 1975; Pozrikidis, 1992). The present model is based on an extension of this theory by Grünbaum (1998) that approximates the velocities and forces generated by ciliated tentacles or arms. In this model, the lateral cilia produce a tangential velocity directed perpendicularly to the axis of the arm and with a speed proportional to the cosine of the angle from the plane of the ciliary bands (see Figs. 2 and 3 of Grünbaum, 1998).

The principle restrictions on the model (in addition to the simplified geometry) are the need to include sufficiently many segments to obtain an accurate approximation of the force distribution on each arm, while at the same time each of those segments must have a high length-to-radius ratio. In some cases, this means that the arms modeled are more slender than the real larval arms. However, our analysis found that variation in arm diameter had a weak quantitative effect on the results, and revealed no qualitative changes in the effects of arm number and orientation as a function of arm radius. This lends confidence that the variation of swimming characteristics observed in very slender-armed geometries also apply to larvae with thicker arms.

Some models in the recent literature have used the full equations of fluid motion (the Navier-Stokes Equations) and grid-based computational methods to investigate flows around large, fast zooplankton (e.g. copepods; Jiang *et al.,* 2002b,a) swimming at

intermediate $\mathcal{R}e$. Compared to those models, the present model is more limited, in that it is restricted to a low-$\mathcal{R}e$ flow regime, and to morphologies which can be usefully approximated with arrays of slender cylinders. The advantage of our approach is that it requires far less computational power. This makes it possible to examine hundreds of larval morphologies—and in cases where swimming trajectories are sensitive to initial posture or are chaotic, hundreds of realizations for each morphology—rather than just a few. Furthermore, because our method does not depend on a grid, larval trajectories can be modeled over larger distances and longer times, in a greater variety of external flows than is feasible with more complex fluid models. The ability to obtain numerous long trajectories allows tests of Hypotheses 1–3 in ways not possible with fewer or shorter trajectories.

All of the larvae considered in this paper achieve stability passively through the center of buoyancy being located anterior to the center of gravity. The stability characteristics of alternative larval geometries were investigated by calculating swimming movements in shear flows. In these flows, either the X-direction velocity was proportional to the Z-direction position, with all other flow components zero (i.e., horizontal shear) or the Z-direction velocity was proportional to the X-direction position, with all other flow components zero (i.e., vertical shear). The simulated larval trajectories in shear were sometimes complex. For example, the three trajectories of model larvae in horizontal shear in Figures 3, 4, and 5 represent successive increases in horizontal shear intensity, through a range in which the passive stability of one larval morphology is overcome by the external fluid motion. The results are qualitative differences in the larva's trajectory: the larva's orientation is constant and its net velocity upward at low shear, while at higher shears the larva loses its ability to maintain an upward posture and a positive upward swimming velocity.

Larval trajectories in vertical shear were even more dramatic (Fig. 6). A larva whose velocity is directed upward in still water is typically inclined off the vertical in the presence of vertical shear. In the inclined larva, what had been strictly vertical swimming has a horizontal velocity component. This component is usually small. Nonetheless, it is highly significant because it is directed toward the downwelling water. As a result, the larva moves into water that is moving downward at progressively more rapid speeds. The larva's own modest upward swimming speed is quickly overwhelmed, and (as illustrated in Fig. 6) the larva plummets at many times its swimming speed. If, as seems likely, the ability to move upward through the water column is an important benefit of swimming, this is potentially a pathological situation. Furthermore, simply swimming faster does not ameliorate the problem—in fact, swimming faster results in faster downward movement—but reducing the tilt off the vertical minimizes it. This can be achieved by increasing passive stabilizing moments (which typically involves the addition or redistribution of weight), as well as by decreasing the "exposure" of the larva to the external shear flow. Hypothesis 2 suggests that some larval morphologies are much more susceptible to this vertical shear effect than others.

The following sections present an attempt to quantify and characterize both larvae's still-water swimming performance and their susceptibility to decreases in that performance

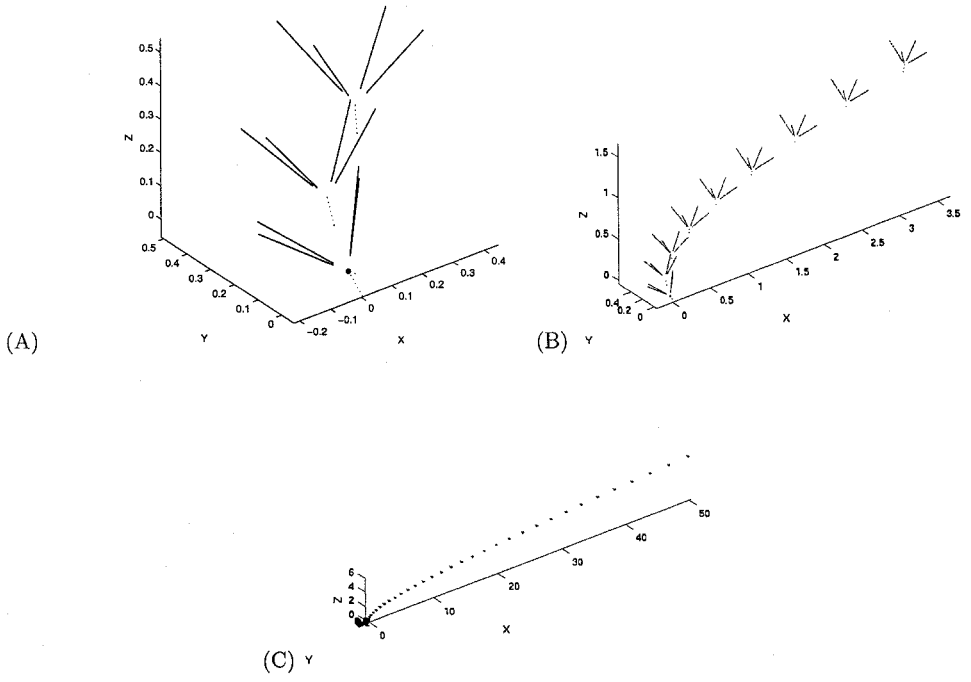

Figure 3. The sequence of positions of a model larva in a relatively weak horizontal shear flow, $U_1 = Z$, $U_2 = U_3 = 0$ (velocity components in the X, Y and Z directions, respectively), are imaged every 0.5 time units. Shown are: (A) a detailed view of initial reorientation and movement ($0 \leq t \leq 1$); (B) the short-term advective transport ($0 \leq t \leq 4$); and (C) the longer-term advective transport ($0 \leq t \leq 16$). At this level of shear, the larva's passive stability maintains a constant angle off the vertical, and the larva is able to swim upward. The body forces are given by $\mathbf{F}_{buoy} = [0, 0, 0.05]$, $\mathbf{X}_{buoy} = [0, 0, 0]$, $\mathbf{F}_{grav} = [0, 0, -0.15]$, and $\mathbf{X}_{grav} = [0, 0, -0.1]$. $V_{cilia} = 1$. The initial position is $\mathbf{X}_L = [0, 0, 0]$, and the initial Euler angles are $\phi = 5.6$, $\theta = -45$, $\psi = 11.25$. In this and succeeding figures, $D_{arm} = 0.00125$, $R_{min} = 0.05$ and R_{max} is chosen to make total arm length equal unity.

due to external shear flows. First, the design criteria are specified that will be used to summarize swimming performance. Then, an attempt is made to decouple the effects of larval *size* from the effects of larval *shape,* by detailing how the performance measures scale with isometric increases in larval size and ciliary velocity. The next section focuses on the specific effects of larval morphology—the number, length and orientation of arms—on the performance measures. Finally, implications of the results for trends and trade-offs in evolution of larval forms are discussed.

3. Swimming performance measures

Larvae must accomplish many different tasks—feeding, avoiding predators and unsuitable environments, locating substrate, etc. In view of these complex requirements, it is impossible to assign a precise relative importance to various aspects of swimming

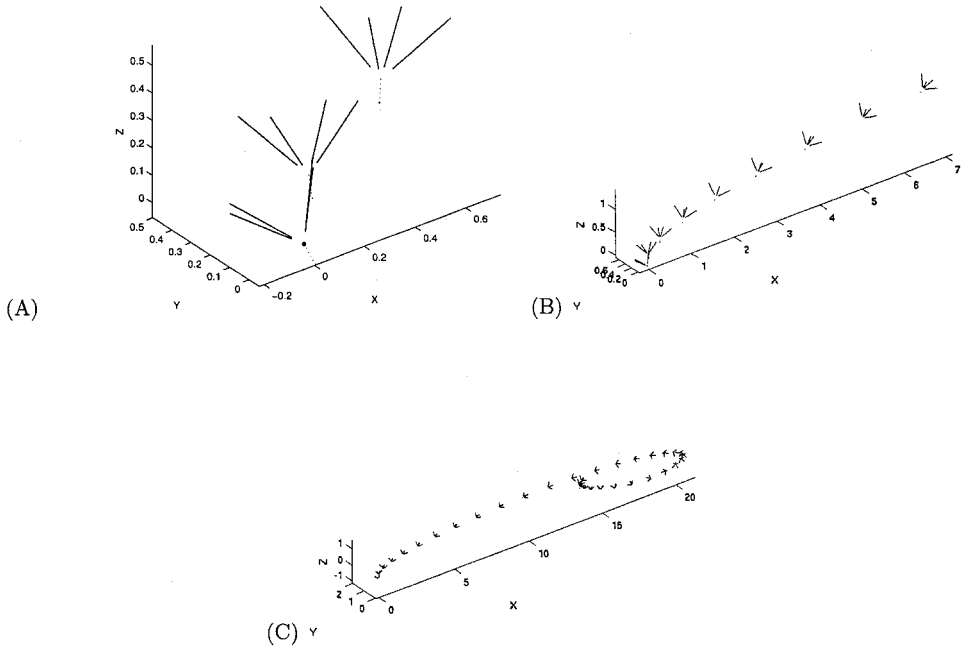

Figure 4. The sequence of positions of a model larva in an intermediate horizontal shear flow, $U_1 = 2Z$, $U_2 = U_3 = 0$, are imaged every 0.5 time units. Other details are as in Figure 3. At this level of shear, the larva's passive stability is insufficient to maintain a constant angle off the vertical, and the larva tumbles end over end.

performance. However, several performance measures reflect characteristics that are probably important for a broad spectrum of larval types under a variety of conditions. This study focused on just a few such performance measures which fall broadly into two types: (i) assessments of larval swimming performance in still water; and (ii) stability assessments that quantify the robustness of swimming performance to external disturbances such as shear or turbulence. These measures are now defined, and some useful relationships between them explained that help interpret their implications for larval morphology.

a. Design criteria for performance in still water

In still water, the swimming velocity of a larva depends on the viscous drag on the body, on ciliary action, and on the strength of the buoyancy and gravity forces. *Swimming speed at neutral weight,* V_{nw}, is defined as the speed at which a larva would travel if gravity and buoyancy forces were absent (i.e., the speed at which the propulsive force of the cilia is equal and opposite to the viscous drag on the body). *Weight capacity* of a larva, F_{wc}, is defined as the maximum net downward force (gravity minus buoyancy) that the larva can sustain at zero velocity. The *sinking speed,* V_s, is defined as the rate of downward movement of a larva bearing a load, F_{wc}, when the larva is in its normal upright position but its cilia are not beating.

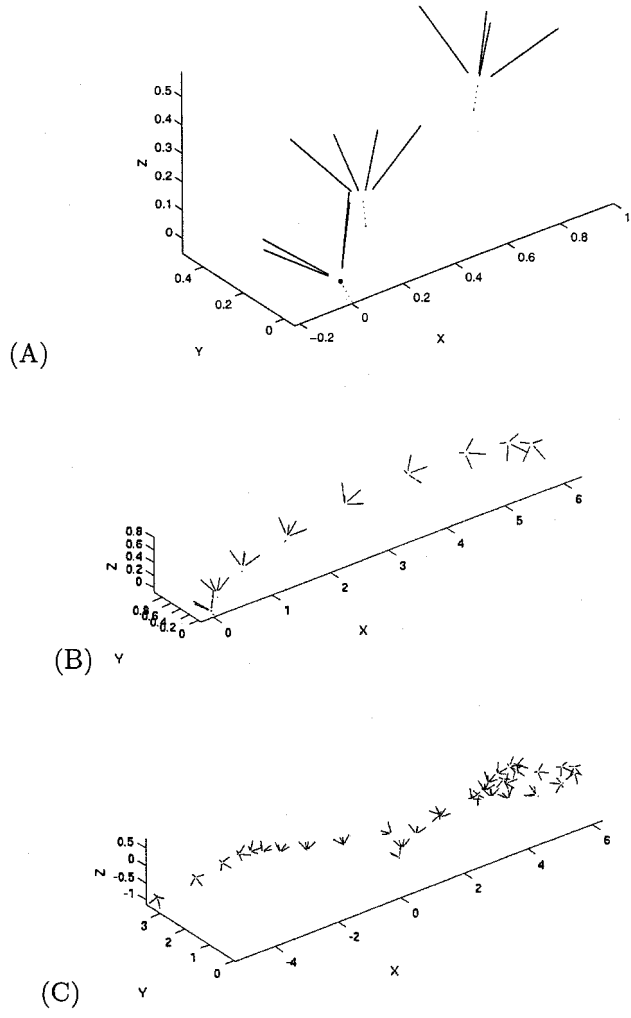

Figure 5. The sequence of positions of a model larva in a relatively strong horizontal shear flow, $U_1 = 3Z$, $U_2 = U_3 = 0$, are imaged every 0.5 time units. Other details are as in Figure 3. At this level of shear, the larva's passive stability is insufficient to maintain a constant angle off the vertical, and the larva wobbles chaotically.

The additive nature of fluid forces at low $\mathcal{R}e$ leads to a number of useful relationships between these performance measures. First, the effect of turning ciliary propulsion on is always to increase forward velocity by V_{nw}, regardless of how a larva is loaded or what is its unpowered sinking speed. Conversely, the effect of turning ciliary propulsion off is always to decrease forward velocity by V_{nw}, no matter what is its powered swimming speed. Therefore, a larva with active cilia that is loaded to its full weight capacity (F_{wc}), and is therefore hovering at zero velocity, will start to sink with velocity V_{nw} when its cilia

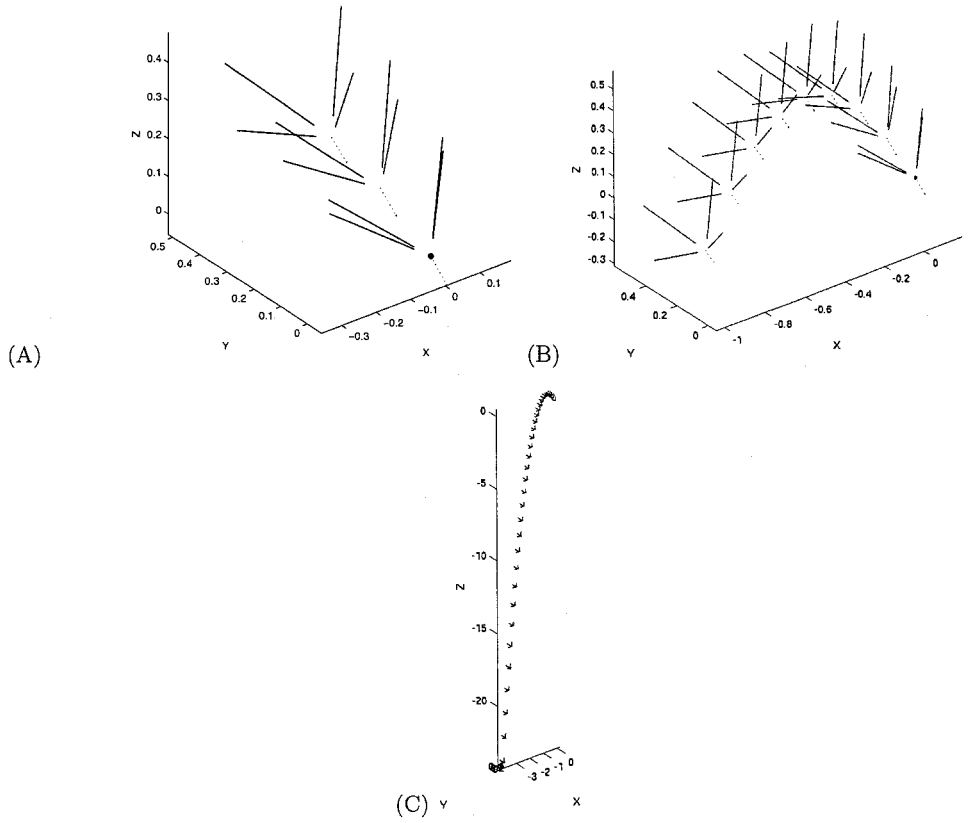

Figure 6. The sequence of positions of a model larva in a vertical shear flow, $U_3 = X$, $U_1 = U_2 = 0$, are imaged every 0.5 time units. Other details are as in Figure 3. The vertical shear pulls the larva off the vertical, giving it a component of velocity into the downwelling water. Thus the larva descends rapidly, despite having a positive upward swimming speed relative to the water in its immediate vicinity.

are inactivated. This implies that $V_{nw} = V_s$. It follows from this that the three still water criteria—V_{nw}, F_{wc}, V_s—represent only two independently variable larval characteristics.

Second, if a larva in still water is bearing a load fF_{wc} (that is, a fraction f of its maximum capacity) then its upward swimming speed is $(1 - f)V_{nw}$ when cilia are beating and its downward sinking speed is fV_s when cilia are not beating. Thus, to maintain a constant range of vertical positions in still water, the larva must spend a fraction f of its time swimming and the rest $(1 - f)$ sinking. Most larvae probably have $0 \leq f \leq 1$ (i.e., they are negatively buoyant but ciliary propulsion is sufficient to swim upward), although some larvae at some times may be positively buoyant, in which case $f \leq 0$.

For some larvae, feeding is apparently equivalent to swimming in terms of ciliary activity, excepting transient reversals of ciliary beat during particle capture. If larvae must swim to eat, and if larvae must at times maintain a roughly constant vertical position in the

water column (e.g. within food layers), then there is a trade-off between time spent eating and time spent sinking. To maximize time spent feeding while maintaining position, a larva of a given morphology should have a weight that brings f close to unity. This would also confer the ability to sink rapidly in the water column, for example to avoid UV radiation (Pennington and Emlet, 1986). However, to maximize ability to move upward in the water column, a larva should have a weight that brings f close to zero. Thus, a trade-off may exist between weight regimes favorable for feeding and downward movement and those favorable for upward swimming. In larvae that feed constantly, this suggests a benefit to having an active reorientation mechanism, that overcomes passive stability to allow active ciliary propulsion in the downward direction, or to segregating cilia into independent feeding and swimming components.

For isometric geometries, the neutral swimming velocity, V_{nw}, is proportional to the ciliary velocity, as parametrized for example by the ciliary tip speed, V_{cilia}. Thus, it makes sense to speak of the *relative neutral weight swimming speed,*

$$V^*_{nw} = \frac{V_{nw}}{V_{cilia}}. \tag{1}$$

The maximum weight capacity is also proportional to V_{cilia}, as well as to the fluid viscosity, μ, and the length of the larva, as for example parametrized by the total length of the ciliary band, L_c. Thus, it makes sense to speak of the *relative weight capacity,*

$$F^*_{wc} = \frac{F_{wc}}{\mu V_{cilia} L_c}. \tag{2}$$

The relative measures V^*_{nw} and F^*_{wc} are *nondimensional* indices, in which the basic dependence on size and speed are scaled out. These measures can be considered "shape factors" that reflect the consequences of a particular geometry.

Putting our results in terms of V^*_{nw} and F^*_{wc} makes them potentially applicable to a wide variety of larvae. For example, for any member of an isometric set of larvae, the swimming speed V in still water with a net body force F_{body} (i.e., weight minus buoyancy) is

$$V = V_{cilia}(1 - f)V^*_{nw},\ f = \frac{F_{body}}{\mu V_{cilia} L_c F^*_{wc}}. \tag{3}$$

Thus, computing values for V^*_{nw} and F^*_{wc} (as we do below) is sufficient to estimate swimming speeds for a wide range of larvae under various loadings and water conditions.

For a set of isometric larvae, a null hypothesis might be that the body forces (weight and buoyancy) increase proportionally to $\rho g L_c^3$, where g is gravitational acceleration and ρ is a characteristic density (e.g., the density of the fluid for buoyancy forces, or the density of the larvae for gravity forces). If that were the case, then these forces would increase more quickly with size than the propulsive force of the cilia (Emlet, 1994). Thus, a reasonable expectation might be that a ciliary geometry which is sufficient to provide control of velocity and position in a small larva could be insufficient for a larger one, even if these larvae have the same shape. These scaling characteristics suggest that larger larvae need

disproportionately more extensive ciliary bands, perhaps enough to maintain a roughly constant proportionality between the body and ciliary forces. This allometry is also that predicted by a roughly constant particle capture rate per unit ciliary band length and per unit body mass (McEdward, 1984; Hart and Strathmann, 1994).

b. Design criteria for stability in shear and turbulence

A larva's ability to maintain a favorable orientation with respect to its surroundings (e.g., upward swimming) is referred to as stability. Stability implies that a larva can return to its preferred orientation after being perturbed by external flows, ciliary reversals, etc. Several aspects of stability in flow could be relevant to larval life histories. A narrow definition of stability might be that a larva always adopts a single, constant orientation in a constant shear field, and that orientation doesn't deviate too strongly with moderate intensities of fluid motion. For example, a "highly stable" larva could orient so as to swim upward in still water and maintain upward swimming despite vertical or horizontal shear. This could be broadened slightly to include cases in which there are multiple such orientations (e.g. the larva adopts and maintains either an upward-directed posture or a downward-directed posture in shear, depending on its initial orientation). Here, a still more general definition of stability is adopted, that includes larvae that may "wobble" or spin in a shear flow, while maintaining a general upward or downward posture that enables them to move in a directed way with respect to their environment.

The mechanisms through which larvae attain stability have been considered (among others) by Mogami *et al.* (2001), who differentiated between stabilizing moments produced by body forces and those produced by hydrodynamic forces. In the present context, the body force moments on isometric larvae are proportional to $\rho g L_c^4$. The moments due to external flow are proportional to $\mu|\nabla U|L_c^3$, where $|\nabla U|$ is the characteristic shear intensity of the flow in the larva's vicinity. The hydrodynamic moments due to ciliary action are proportional to $\mu V_{cilia} L_c^2$. Thus, it makes sense to describe moments nondimensionally as

$$M^*_{body} = \frac{M_{body}}{\rho g L_c^4}, \quad M^*_{flow} = \frac{M_{flow}}{\mu|\nabla U|L_c^3}, \quad M^*_{cilia} = \frac{M_{cilia}}{\mu V_{cilia} L_c^2}, \tag{4}$$

where M_{body}, M_{flow} and M_{cilia} represent the magnitudes of their respective moments. As in (1), M^*_{body}, M^*_{flow} and M^*_{cilia} are nondimensional shape factors, with basic dependencies on L_c, V_{cilia}, ρ and μ scaled out. Among an isometric set of larvae, body moments increase more rapidly with L_c (proportional to L_c^4) than do moments from external or self-generated flows (proportional to L_c^2 or L_c^3). Therefore, we expect that isometric larvae which are passively stabilized by body forces (center of buoyancy anterior to center of gravity) are more able to resist shear flows as they become larger. In combination with the previous arguments, this suggests that for larger larvae, morphological traits favoring rapid feeding and weight-bearing capacity may be more important and those favoring stability may be less important, relative to those same traits in smaller larvae.

A larva with a fixed orientation in a shear flow passively stabilized by body force moments has

$$\mathbf{M}_{body} + \mathbf{M}_{flow} = 0.$$

From this it follows that isometric larvae of different sizes or immersed in different shears are dynamically similar if

$$\frac{M^*_{flow}}{M^*_{body}} \propto \frac{\rho g L_c}{\mu |\nabla U|}. \tag{5}$$

In (5), the shape factors on the left-hand side (and the constant of proportionality) are constant among any set of isometric larvae. Eq. 5 provides a means of inter-comparing passive larval stabilities across various situations. For example, if a larva doubled its size (L_c) isometrically, its passive stability would be equivalent if either the strength of shear or the viscosity were also doubled, or if the density differences were halved. The constant of proportionality in (5) varies with the orientation of the shear.

As will be seen, movements of larvae in shear—and therefore the design criteria to optimize these movements—differ in important ways between horizontal and vertical shear flows. In particular, the pathological effect illustrated in Figure 6 has a dependence on the intensity of vertical shear that is stronger than linear. If the vertical shear is not too strong, the horizontal speed of the larva toward downwelling water is expected to be proportional to shear intensity (this is consistent with model results presented below). The rate of increase of downward velocity of the fluid with distance is also proportional to shear intensity. Thus, the larva experiences a downward acceleration proportional to the vertical shear intensity squared.

4. Performance compromises and shape

Given a length of ciliary band required for feeding, how should that ciliary band be allocated to maximize swimming performance? Swimming performance in still water was calculated for a series of larval geometries, with different allocations of a fixed total arm length to varying numbers of arms with various elevation angles (Fig. 7). For all arm numbers, relative neutral-weight speed (V^*_{nw}) was maximal for flat geometries ($\alpha = 0°$), but did not fall off substantially until arm angle exceeded approximately 45°. For arm angles below 45°, the number of arms had little effect. However, for acute angles (>60°), V^*_{nw} decreased rapidly with decreasing numbers of arms. For these acute angles, geometries with larger numbers of arms swam slightly faster than those with few arms.

Relative weight capacity (F^*_{wc}) decreased as a function of arm angle. This reduction was quite small until above approximately 30°, but weight capacity declined dramatically for large α. For all arm angles, geometries with more and shorter arms had lower weight capacity than geometries with fewer and longer arms. This reflects interference between larval arms when they are too close—ciliary propulsion on one arm induces a "downdraft" in its vicinity, exerting a downward force on other arms within this flow. Larval morphologies with few arms at low elevations minimize these adverse hydrodynamic interactions between arms, and therefore enhance weight capacity.

The calculations in Figure 7 summarize larval swimming performance for each of these

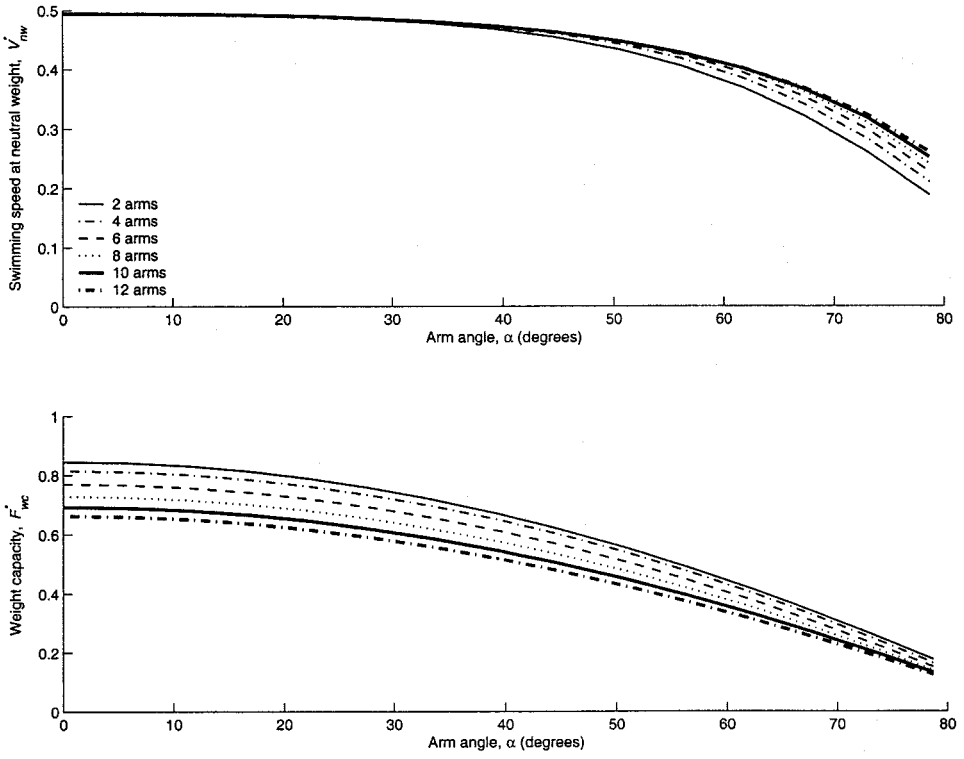

Figure 7. For each larval geometry, the total length of ciliary band is $L_c = 2$; thus, the total lengths of the arms is equal to unity in all cases. This figure summarizes the consequences for relative neutral-weight speed (V^*_{nw}) and relative weight capacity (F^*_{wc}) of allocating that total arm length equally among various numbers of arms, and positioning those arms at various elevation angles (α). See Eqs. (1) and (2) for details. Elevation angle $\alpha = 0°$ represents a flat arm geometry in which arms lie in the XY plane, with ciliary propulsion acting in the positive Z-direction. Elevation angles near $\alpha = 90°$ represent arms approaching vertical; ciliary forces on each arm then have large horizontal components.

geometries with the use of Eq. (3). These results are summarized in Table 1. With respect to Hypothesis 1, Table 1 suggests that larval forms differ substantially in swimming speed and weight capacity in still water, suggesting that selection on these traits may constrain the evolution of morphological traits.

A related question is, what is the payoff in swimming performance for adding additional ciliary band length? This question was addressed by extending the arms on larvae from Figure 7 for a single elevation angle ($\alpha = 45°$) and for several numbers of arms. The resulting curves are presented for V^*_{nw} and F^*_{wc} in Figure 8. For an isometric enlargement, V^*_{nw} and F^*_{wc} would not change, implying that speed was unaffected and weight capacity was proportional to L_c. Lengthening arms is not an isometric enlargement because the arm diameter and the basal radius (R_{min}) do not change in proportion. Nonetheless, the changes

Table 1. Consequences of larval morphology for performance.

Measure	Functional trends	Optimization strategies
Neutral weight speed, V^*_{nw} (Fig. 7)	Decreases at high arm elevations (α); advantage to more and shorter arms, but only at very high arm elevations.	Low arm elevations.
Weight capacity, F^*_{wc} (Fig. 7)	Decreases at medium and high arm elevations (α); advantage to fewer and longer arms, especially at low arm elevations.	Low arm elevations and few arms.
Stability in horizontal shear (Fig. 9)	Advantage to 2- or 12-arm (but not intermediate) morphologies at low arm elevation; otherwise, advantage to many arms at high elevation angles.	Many arms with high or low (but not intermediate) elevation angles, or two arms with low elevation angles.
Stability in vertical shear (Fig. 10)	Advantage to high arm elevations with 2 or 12 arms.	High arm elevations and 2 or 12 but not intermediate numbers of arms.

in V^*_{nw} and F^*_{wc} in the simulations are small. This indicates that predicted swimming performance is not strongly sensitive to arm diameter or R_{in}.

In view of the different moment scaling relationships (Eqs. 4) and the many possible ways of quantifying larval swimming stability, this study used what appeared to be the simplest and most general. Stability in horizontal shear flows was characterized by measuring the vertical distance traveled by a larva in a fixed time in each flow in Figure 9. Similarly, stability in vertical shear flows was characterized by measuring horizontal movements (for larvae that would be swimming directly upward in still water) in Figure 10. The simulations in these figures represent a single configuration of weight and buoyancy distributions. The specific quantitative results would differ for other weight and buoyancy distributions; however, the qualitative trends in these figures probably typify a wide range of possible configurations. The horizontal axes in these figures represent the relative intensity of horizontal shear, $(\partial U_1/\partial Z)^* = (\mu/\rho g L_c)(\partial U_1/\partial Z)$, and vertical shear, $(\partial U_3/\partial X)^* = (\mu/\rho g L_c)(\partial U_3/\partial X)$, respectively. Because the trajectory of a larva in our simulations depends in some cases on its initial orientation, this measurement is repeated many times for each morphology and each shear intensity, with different randomly chosen initial orientations. The resulting distribution of vertical and horizontal movements is then informative not only about the sensitivity of a larval geometry to shear but also about the degree to which multiple stable orientations may lead to wildly divergent trajectories among a cohort of similar larvae.

Figures 9 and 10 suggest that larval forms differ in their susceptibility to being destabilized by shear flows, and that furthermore the most stable morphologies differ

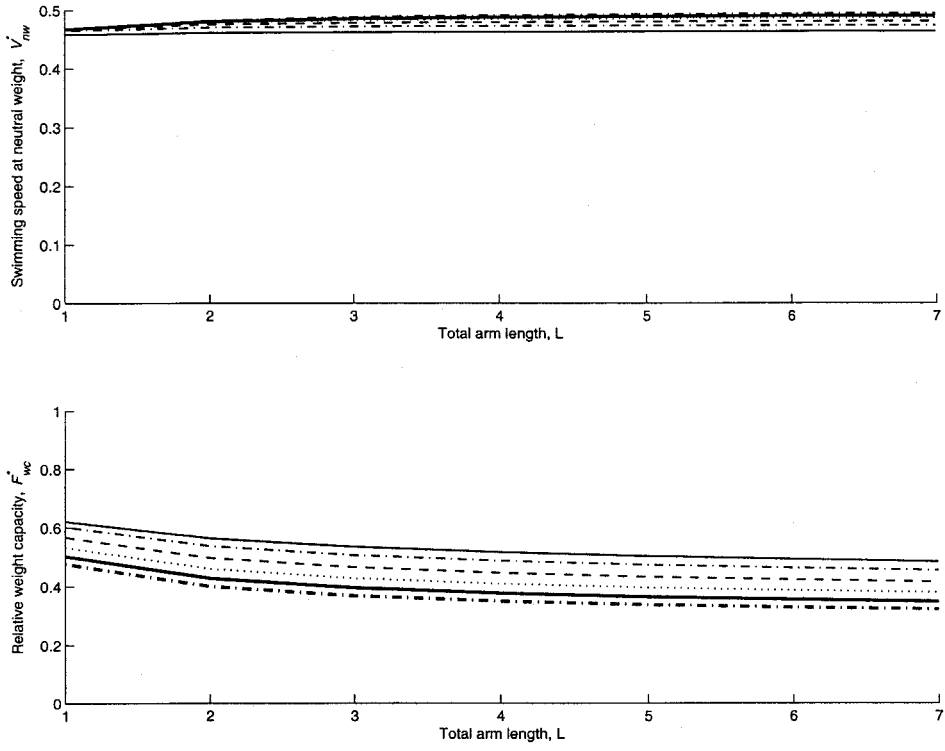

Figure 8. This figure shows the effect of increasing total arm length (L_c) on the scaled performance measures, V^*_{nw} and F^*_{wc}. Over a seven-fold increase in total arm length, performance changes relatively little. Note that this implies a nearly linear dependence of weight capacity, and almost no dependence of swimming speed, on the corresponding unscaled performance measures, V_{nw} and F_{wc}, as arms are lengthened while other geometrical characteristics are kept constant. Line definitions are as in Figure 7.

between horizontally and vertically oriented shear. In horizontal shear, several possible morphologies seem to perform adequately, including some with low arm elevations that conferred high swimming speeds and weight capacities (Table 1). However, only a small subset of larval morphologies performed well in vertical shear, and none of those had low arm elevations. With respect to Hypotheses 2 and 3, this suggests that larval morphologies differ in ability to maintain stability in external shear flows, and furthermore that, to the extent selection is acting on the ability to maintain orientation and swimming direction, enhancing performance in shear may constrain larval swimming speed and weight capacity.

5. Implications for ecology and evolution of armed larvae

The model demonstrates that the number and elevation of arms with ciliary bands matters for performance in swimming. The model examined only radially symmetrical

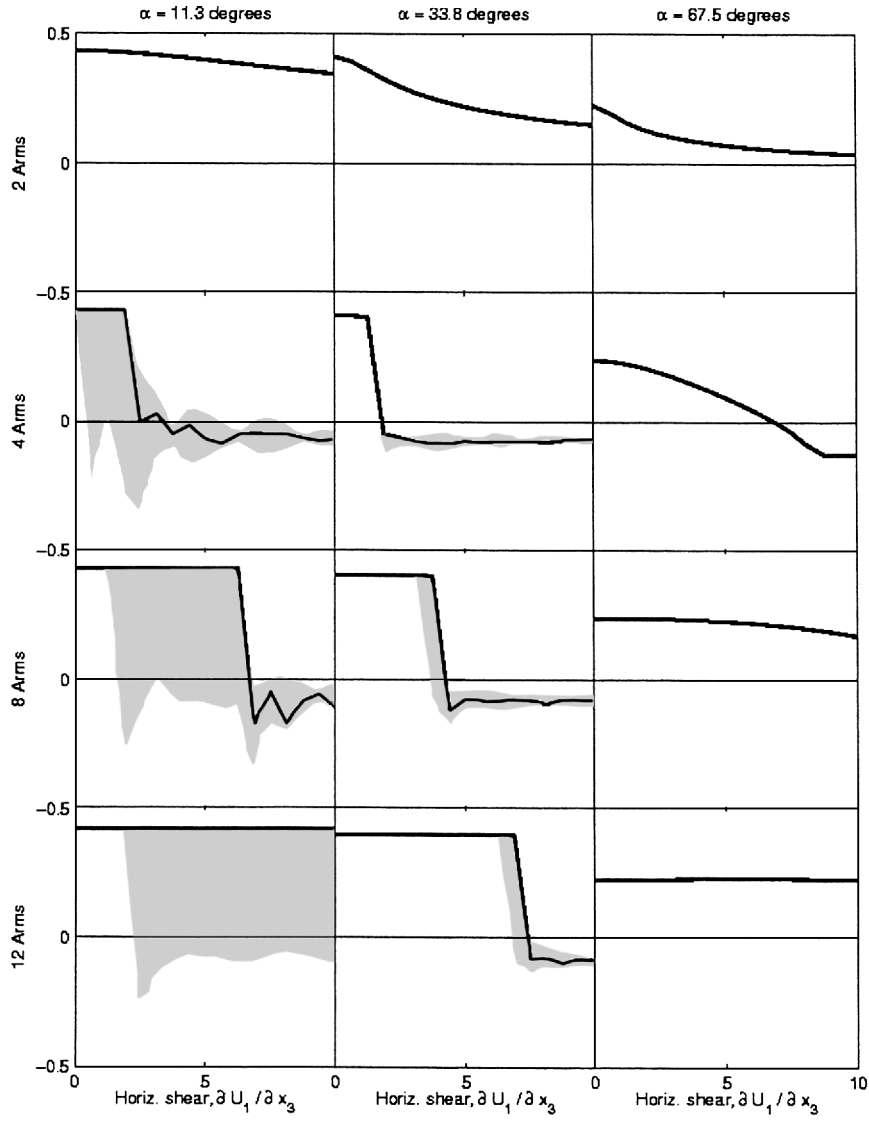

Figure 9. This matrix of plots summarizes 24576 simulated trajectories in horizontal shear. Each row represents a fixed number of arms, and each column represents a fixed arm elevation angle. Within each plot, the horizontal axis represents the relative intensity of horizontal shear, $\partial U_1^*/\partial Z$. The vertical axis represents the average upward velocity over a fixed time interval after initial transients have passed ($t = 100$ to $t = 120$). Solid lines represent the median velocity of 128 larval trajectories, each starting from different random initial orientations at each of 16 shear intensities. Shaded areas represent 10th and 90th percentiles of vertical velocity. Negative values imply that larvae sank during the interval. In all cases, $F_{buoy} = [0, 0, 0.05]$, $X_{buoy} = [0, 0, 0]$, $F_{grav} = [0, 0, -0.15]$, and $X_{grav} = [0, 0, -0.1]$.

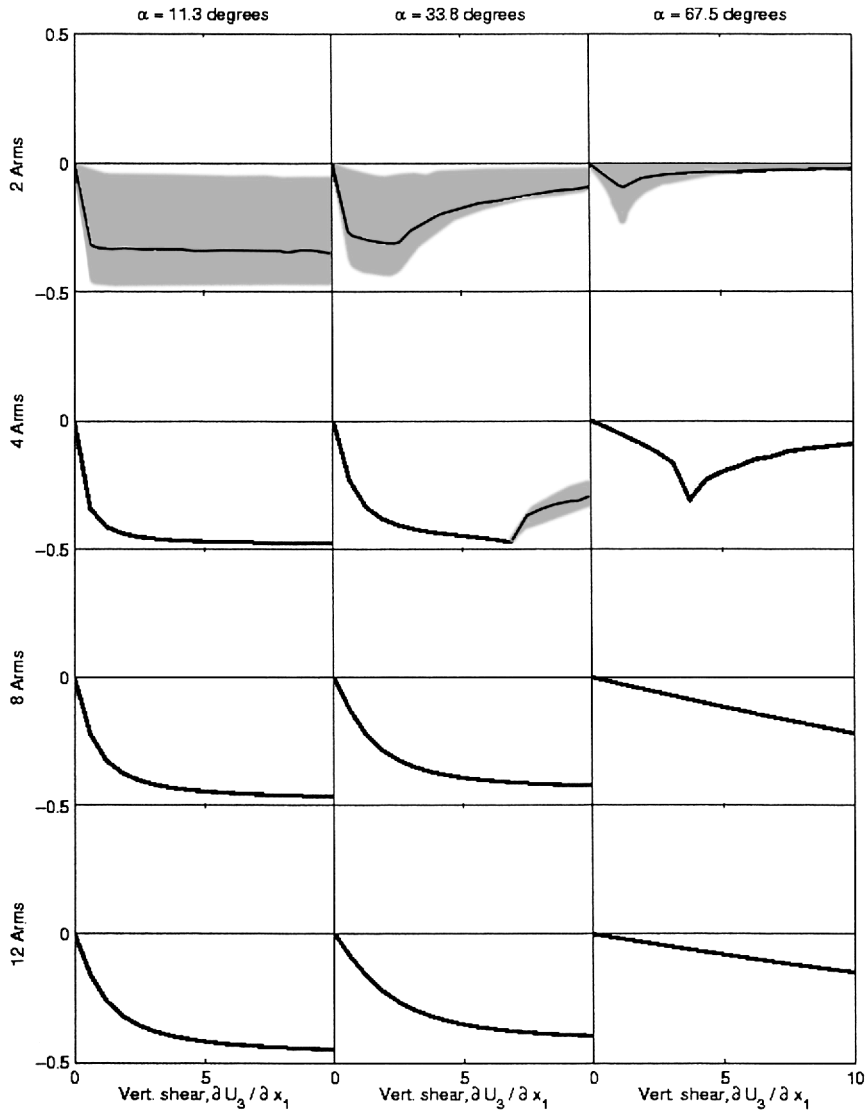

Figure 10. This matrix of plots summarizes 24576 simulated trajectories in vertical shear. Within each plot, the horizontal axis represents the relative intensity of vertical shear, $\partial U_3^*/\partial X$. The vertical axis represents the average horizontal velocity over a fixed time interval after initial transients have passed ($t = 100$ to $t = 120$). Negative values imply that larvae moved toward downwelling water during the interval. Other details are as in Figure 9.

arrangements of arms of equal length; only the arm cilia contributed to swimming; and ciliary beat was constant. These simplifications aided interpretation of results, yet the model is close enough to existing larval forms to permit predictions and comparisons. Here are implications.

One prediction of the model is that there is no single arrangement of arms that maximizes performance in speed, weight capacity, and stability in swimming (Table 1). Low arm elevations performed well in most respects, providing greater speed, greater weight capacity, and stability in horizontal shear. However, in vertical shear, lower arm elevations resulted in greater movement into downwelling water. Movement into downwelling water would likely result in downward transport in turbulence, which could be disadvantageous for larvae that are not ready to settle. Other arm arrangements, outside the range examined here, can avoid this downward bias in vertical shear (Grünbaum and Strathmann, unpub. obs.), but it is clear that out of a wide range of numbers and elevations of arms, no one arrangement performed maximally for all criteria for swimming. No arrangement of arms, tentacles, or lobes is optimal for all requirements of speed, weight capacity, and stability.

Existing larvae differ in number and elevation of arms and presumably represent different compromises among performance criteria. Even among plutei there are striking differences in elevation and number of arms with development and among species. The model predicts corresponding differences in speed, weight capacity, and stability in shear. Steadily swimming armed larvae experience the same body of water differently, depending on their form.

All modeled forms moved into downwelling water in vertical shear (Fig. 10). Consistent with this prediction, the 8-armed larvae of *Dendraster excentricus* (Fig. 1) moved from upwelling to downwelling currents in vertical shear (Strathmann and Grünbaum, unpub. obs.). An implication is that in turbulence, the larvae would move into the downward moving parts of turbulent eddies. Curiously, weighting for passive stability with an upward orientation can contribute to downward movement. High arm elevations decreased this motion but also had lower speed and weight capacity (Fig. 7) and decreased upward swimming in horizontal shear, where low arm elevations performed better (Fig. 9). One possible way to enhance stability in shear would be changes in ciliary beat to adjust orientation of the larva. The modeled larvae are swimming automata, whereas real larvae can alter ciliary beat. However, there has been no demonstration that changes in ciliary beat reorient larvae that have been tilted in shear. Departures from radial symmetry in the modeled larvae are another means of avoiding the movement into downwelling water (Grünbaum and Strathmann, unpub. obs.). It remains to be seen whether larvae solve problems of stability and vertical motion by traits excluded from the model. Either the identified effects of shear are not fatally disadvantageous, or the problems are solved by other means.

These results are the bad news for anyone wishing to design armed larvae. The good news is the small effect of arm elevation and arm number on speed and weight capacity (Fig. 7). Sufficient performance, as opposed to maximal performance, may be obtained within a wide range of larval forms. Put another way, other functional requirements, such as feeding or defense, may affect selection on arm elevation or arm number.

6. Comparison of larvae to predictions

Additional good news is that other features of larvae can compensate for the deficiencies of arms as structures for swimming. The taxonomically diverse echinoplutei in Mor-

tensen's (1921) plates provide a sample of larvae in the 4 to early 8-arm stages, all with the long postoral arms in fixed positions. The postoral arms are initially the longest and usually have lower elevations than the anterolateral arms (Fig. 1). Of 14 species in 4 orders, 11 had elevations of postoral arms between 60 and 70°, although two species of *Toxopneustes* had lower arm elevations of 44 and 56° and one *Strongylocentrotus* species had an arm elevation as high as 80°. At elevations above 60°, speed and weight capacity decline markedly (Fig. 7). The disadvantages for speed and weight capacity may be countered in several ways.

First, although arms of plutei are initially fixed in one position, some echinoplutei have moveable arms at later stages, when four of the arms can be swung from high to low elevations (Mortensen, 1921, 1938). Lowering the arm elevation could produce greater speed and weight capacity (Fig. 7). Changing arm elevations could also affect stability, thereby adjusting motion in horizontal or vertical shear. Some echinoplutei of the Diadematidae develop two very long arms, approximating the 2-armed model larvae. At low arm elevations, they would maximize speed and weight capacity (Fig. 7). In published photos, these larvae have lower arm elevations than other echinoplutei (27 and 41°) but the elevations usual in swimming larvae could be different (Eckert, 1998). The arms can be moved from a horizontal position (0°) to a vertical and parallel position (near 90°). Movement of arms in response to shear has not yet been examined. Spreading arms could also be a defense against predators (Emlet, 1983).

Second, echinoplutei have nearly transverse bands between the arms. These bands (with approximately 0° elevation) presumably enhance speed and weight capacity. In some sea urchin species, transverse bands (epaulettes or lobes) develop as the heavy rudiment of the juvenile sea urchin develops. In *Strongylocentrotus* species, the development of epaulettes is associated with an increase in swimming speed (H.-t. Lee, 1983). Although lower speeds and weight capacity are predicted for plutei with high arm elevations, late-stage changes in other ciliary bands of echinoplutei occur when there is a greater requirement for weight capacity in carrying the juvenile rudiment and possibly a requirement for greater speed during settlement.

Third, the high arm elevations of most echinoplutei may reduce movement into downwelling water in vertical shear (Fig. 10), though they are predicted to reduce stability in horizontal shear. For echinoplutei, speed and weight capacity provided by moveable arms and transverse bands are features that can compensate for arm elevations that reduce effects of vertical shear.

The ophioplutei are closer than echinoplutei to the simple armed forms of the model, and the model appears to explain differences among ophioplutei. In contrast to sea urchin larvae, two of the arms of ophioplutei of brittle stars are decidedly longer than the others. In extreme cases, the ophioplutei approximate the modeled two-armed larvae (e.g., *Ophiothrix fragilis,* Fig. 11). The two long (posterolateral) arms often have lower arm elevations than the arms of echinoplutei. Elevations of the posterolateral arms can be as low as 15° or range as high as 70° distally (Mortensen, 1921, 1931, 1937). The model predicts greater speed and weight capacity for those ophioplutei that have long posterolateral arms with

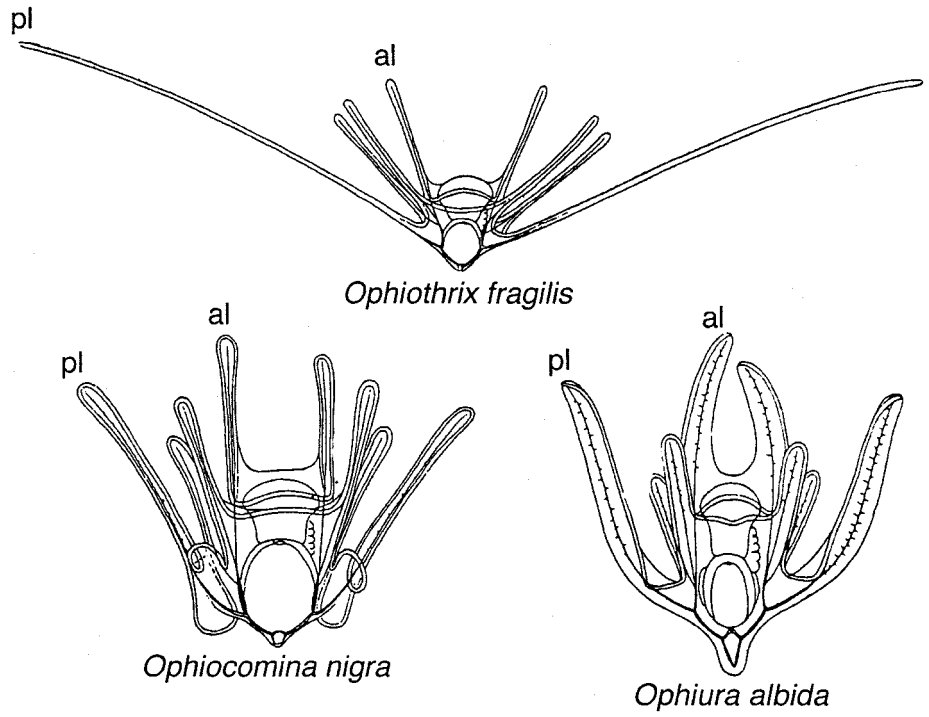

Figure 11. *Ophiothrix fragilis* and *Ophiocomina nigra* retain their posterolateral arms at metamorphosis. *Ophiura albida* resorbs its posterolateral arms at metamorphosis. *O. nigra* is the anomalous larva in Figure 12, and an inferred independent evolution of retention of posterolateral arms through metamorphosis. Images modified after Mortensen (1927b).

low elevations (Fig. 7). The model predicts greater stability in shear for those ophioplutei with arms more nearly equal in length and at higher elevations.

These predictions for performance in swimming are consistent with patterns of arm resorption at metamorphosis (Hendler, 1991; Byrne and Selvakumaraswamy, 2002). In one type of metamorphosis, all but the posterolateral arms are resorbed as the juvenile brittle star develops. Only the posterolateral arms remain, and these carry the juvenile (as occurs in *Ophiothrix fragilis,* Fig. 11). In the other type of metamorphosis, all arms are resorbed, though often with the posterolateral and right anterolateral arms later than the others (as occurs in *Ophiura albida,* Fig. 11). In some that resorb all arms at metamorphosis, portions of the ciliary band remain and are rearranged to form nearly transverse bands. The expectation from the model was that lengths and elevations of posterolateral arms would differ with type of metamorphosis because demands on the posterolateral arms differ. Figure 12 compares relative arm lengths (ratio of mean length of posterolateral arms to right anterolateral arms) and elevations of the posterolateral arms. As expected from the model, it is the ophioplutei that retain posterolateral arms through metamorphosis that commonly approximate a 2-armed larva with low arm elevations. Those that resorb all

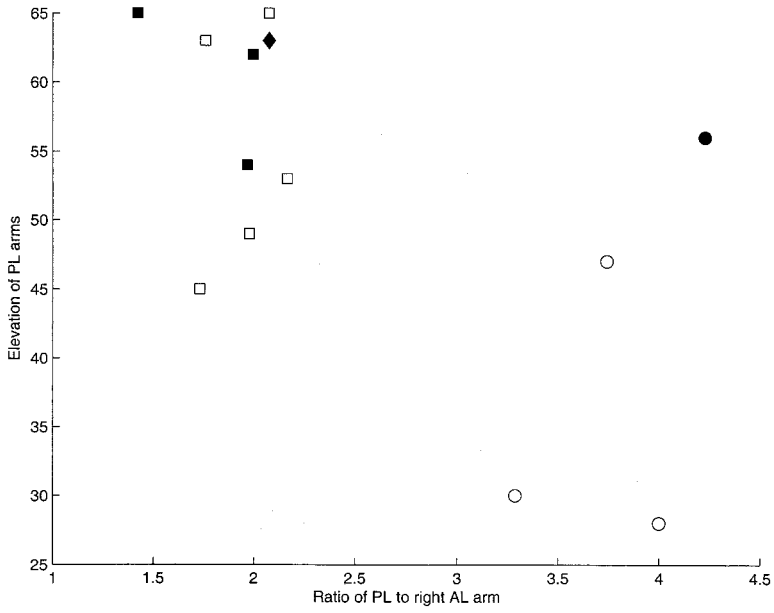

Figure 12. Elevation of posterolateral arms (in degrees) versus the ratio of posterolateral (PL) arm length to anterolateral (AL) arm length. The PL arms tend to have lower elevations and greater length relative to other arms in ophiuroids that retain the PL arms through metamorphosis (circles) than in those that resorb all arms during metamorphosis (squares). The anomalous larva *Ophiocomina nigra* (diamond) is inferred to have evolved retention of PL arms independently of the others. Filled symbols represent larval forms known to possess additional ciliated structures (besides the arms) that may provide additional speed and/or weight-bearing capacity. These include ciliated lobes between bases of arms, an extra small armlet near the base of the PL arm, or rearrangement of ciliated bands into rings. Presence or absence of such structures is not known for all species, so the plot may underrepresent their prevalence. A possible implication is that lobes, armlets, and transverse bands are compensatory structures that enhance speed and weight capacity.

arms at metamorphosis tend to have higher arm elevations, and their posterolateral arms are less elongated relative to their other arms. In other words, those that resorb all arms at metamorphosis are more similar to echinoplutei in form, and like echinoplutei, some rely on transverse portions of the ciliary band rather than arms to carry the developing juvenile.

Measurements of ophioplutei at equivalent stages were obtained from Hendler's (1991) figures and list of types of metamorphosis, and additional figures of advanced larvae that had not yet resorbed arms, preferably ones in which the hydrocoel had formed lobes (Müller, 1851; Mortensen, 1921, 1927a, 1931, 1937; Thorson, 1934; Strathmann, 1971; Mladenov, 1985). Some larvae that retain posterolateral arms through metamorphosis, *Ophiothrix fragilis* and *Ophiomaza cacaotica* (Mortensen, 1927a, 1937) were depicted with lower elevations of posterolateral arms at later stages, when these were the only remaining arms and the juvenile had grown large. The nonfeeding larva of *Ophiothrix oerstedi* was excluded because the only arms to develop are the posterolateral arms

(Mladenov, 1979), but it has a low arm elevation (26°), like most others that retain posterolateral arms through metamorphosis. Positions and relative lengths of posterolateral arms may be highly conserved, however. If resorption of all arms at metamorphosis was ancestral, then retention of posterolateral arms through metamorphosis may have evolved as few as two times in this set of species, given inferred relationships (Smith *et al.,* 1995). Moreover, one of these inferred evolutionary divergences is the anomalous point in Figure 12 for *Ophiocomina nigra* (Fig. 11), which did not evolve relatively long posterolateral arms of low elevation.

The prediction that long posterolateral arms with low elevations provide greater speed and weight capacity is also consistent with the presence or absence of transverse portions of the ciliary band, such as lobes at the base of arms (e.g., *Ophiocomina nigra,* Fig. 11) or rearrangements into transverse bands at metamorphosis. Transverse bands are more extensive and common among ophioplutei with high elevations of posterolateral arms than among those with low elevations (Fig. 12). An apparent exception in Figure 12 is a pluteus with relatively long posterolateral arms that was grouped with those with additional transverse bands (dark filled circle on right). This pluteus does not have lobes or transverse rings, however, but rather small armlets near the base of the posterolateral arms (Mortensen, 1921).

According to the model, ophioplutei that approximate a 2-armed larva with low arm elevation should have a greater tendency to move into downwelling water in vertical shear than would plutei with either 2 or numerous long arms of high elevation (Fig. 10). The arm elevations of ophioplutei like *O. fragilis* are low enough for upward swimming in horizontal shear but not low enough for maximal upward swimming (Fig. 9). Movement into downwelling water in vertical shear could be disadvantageous at early stages, but advantageous later, at settlement and metamorphosis. The model suggests that advantages of movement in vertical shear may account for the high arm elevations of some ophioplutei, while those that evolved long posterolateral arms of low elevation traded those advantages for weight capacity in carrying the developing juvenile.

Other larval forms swim with ciliated bands on tentacles or narrow lobes that are extended with nearly 0° elevation or in some cases angled rearward (with a negative elevation). These forms include the larvae of brachiopods, phoronids, and some gastropods (Young, 2002). The actinula larvae of trachyline medusae also have ciliated arms in this position. These larvae contrast with plutei in having "arms" that are flexible rather than rigid. According to the model, the low tentacle elevations enhance speed and weight capacity of these larvae (Fig. 7) but increase movement into downwelling water in vertical shear (Fig. 10). In these larvae, however, there is a trailing larval body that would influence motion in shear. Also, in neither the brachiopod nor the phoronid are the larval tentacles symmetrically positioned. For the brachiopod larvae and some gastropod larvae, the tentacles or lobes are the sole means of swimming and the larval shell contributes weight that must be carried. The phoronid larvae lack a shell and possess an additional transverse ciliary band for swimming. The demands on the brachiopod larva's tentacles and gastropod

larva's lobes for speed and weight capacity are presumably greater than for the phoronid larva's tentacles, though both have a low elevation.

The model employed four criteria for performance in swimming. The importance of these criteria for performance varies among larvae with stage of development and among species, and other criteria may also be important. Weight capacity may be more important for larvae that are carrying a heavy juvenile skeleton than for larvae at earlier stages, but weight contributes to passive gravitational stability even at early stages (Pennington and Strathmann, 1990). Slow speeds may be adequate for planktonic larval life. A feeding larva requires little speed to avoid the water that it has already cleared of food. Requirements for speed may increase at settlement, however. Some larvae transform to faster forms as they become competent to settle: the doliolaria is faster than the auricularia (Strathmann, unpubl. obs.) and echinoplutei gain speed with epaulettes (H.-t. Lee, 1983). The criteria for stability assumed that maintaining a direction is important, and the discussion assumed that maintaining an upward direction is important. The buoyancy associated with large echinoderm eggs (Kelman and Emlet, 1999; Villinski *et al.,* 2002) and the early upward swimming of embryos with pelagic development (Staver and Strathmann, 2002) suggest that maintaining an upward motion is important, at least at early stages. The performance criteria were for steady swimming, not maneuvering in response to stimuli.

Although a limited set of forms and performance criteria were examined, they were sufficient to pose testable, quantitative hypotheses on larval forms and performance. Differences in number and elevation of arms in the simple modeled forms approximate existing larvae. No one arrangement of larval arms performed maximally by all criteria. Arm angles of most plutei are not maximizing speed or weight capacity. The association of high arm elevations with compensatory ciliary bands in echinoderm plutei is expected from the model. Among ophioplutei, the association of low elevations of posterolateral arms with retention of these arms through metamorphosis is a predicted adaptation for weight capacity in carrying the juvenile. The nearly horizontal tentacles and lobes of larval brachiopods, phoronids, gastropods, and trachyline medusae appear to be well adapted for speed and weight capacity. The existing diversity in larval forms indicates diversity in performance.

7. Implications of passive stability of swimming larvae

The model also pointed to an apparently general deficiency in performance: the motion of a passively oriented swimmer into downwelling water in vertical shear. This consequence of passive stability was predicted in the model for armed larvae, but could apply to diverse planktonic organisms, not just those with arms. A swimmer with passive upward orientation is tilted by shear and swims in the direction of the tilt. In vertical shear, this tilt can move an upward swimming organism away from upward currents and into downward currents. This would occur in the shears produced by turbulence, as well as in larger scale flows such as convergence and divergence zones.

Movement into downwelling water could seriously compromise upward swimming by planktonic animals, or even make it counter-productive. This consequence of passive

stability might be avoided by behavioral responses to shear or evolution of body shape. Shapes other than those considered in this paper appear possible (i.e., larvae with unequal arms) that selectively move into upwelling rather than downwelling water (Grünbaum and Strathmann, unpub. obs.). For larvae and other planktonic organisms that can sense the direction of gravity, selective movements within turbulent eddies provide a possible mechanism whereby turbulence might be exploited for enhanced upward or downward transport. However, many larvae appear neither to adopt upward-biased shapes nor to sense the direction of gravity. For swimmers that do not avoid it, downward movement in vertical shear might be used to advantage or might not be fatally disadvantageous. Further modeling and observations of passively stable swimmers in shear will demonstrate whether this potential deficiency is commonly circumvented or is widespread.

Previous studies suggest that turbulence affects vertical distributions of plankton within the water column and their rates of encounter with predators, prey and substrate. The density of plankton in the uppermost parts of the water column is sometimes observed to decrease with increasing turbulent intensity, possibly through depletion by turbulence-enhanced predation rates or by active avoidance (Franks, 2001; Visser *et al.,* 2001). Theoretical analyses of encounter rates usually predict enhanced encounter rates (Rothschild and Osborn, 1988; Eckman, 1990; Lewis and Pedley, 2000), though capture rates may either increase or decrease (Sundby, 1997; Fiksen *et al.,* 1998; MacKenzie and Kiorboe, 2000). These analyses usually assume independence between swimming motions and turbulent transport. Our model results suggest that, for armed larvae at least, estimates of turbulent effects may need to reflect biased movements within specific parts of turbulent structures. Biased movements may alter both the distribution of movement directions, and also may result in accumulation of larvae in specific parts of turbulent eddies, both of which may affect larval encounter rates (Yamazaki *et al.,* 2002). The predicted downward transport of armed larvae in shear suggests a mechanism by which these larvae may avoid upper layers in the presence of turbulence, or may increase contact rates with benthic substrates. This mechanism may be constitutively "designed into" larvae similar to those we modeled, and therefore may be influencing vertical distributions of these larvae even when they lack gravity sensors that would allow them active downward swimming.

Acknowledgments. This work is an outgrowth of a course on larval biology at Friday Harbor Laboratories. We are grateful to our co-instructors, C. M. Young and J. R. Hoffman and to our students for stimulating discussions, and to FHL's staff and director, A. O. D. Willows, for making it possible. We thank P. Selvakumaraswamy and M. Byrne for information on ophioplutei. The authors gratefully acknowledge support by National Science Foundation grants OCE 0217304 (RRS) and OCE-0220284 (DG).

APPENDIX

Details of model derivation

Dynamics in the model are based on Newton's Second Law, which states that the sum of forces on a body is equal to that body's rate of momentum change. This can be written for a swimming larva as

$$m_L \dot{\mathbf{V}}_L = \mathbf{F}_{cilia} + \mathbf{F}_{ext} + \mathbf{F}_{trans}(\mathbf{V}_L) + \mathbf{F}_{rot}(\mathbf{\Omega}_L) + \mathbf{F}_{body} \approx 0. \quad (6)$$

In (6), the rightmost term represents the assumption that the larva's mass m_L is so small that the inertia of the larva (and of the fluid immediately surrounding it) is negligible. The larva's instantaneous translational and angular velocities ($\mathbf{V}_L$ and $\mathbf{\Omega}_L$) are then determined by (6) as a quasi-steady balance of the component forces: $\mathbf{F}_{cilia}$, the force imparted by the fluid upon the larva due to ciliary action; $\mathbf{F}_{ext}$, the force imparted by the fluid upon the larva due to external flow; $\mathbf{F}_{trans}$, the force imparted by the fluid upon the larva due to the larva's translational velocity, $\mathbf{V}_L$; $\mathbf{F}_{rot}$, the force imparted by the fluid upon the larva due to the larva's rotational velocity, $\mathbf{\Omega}_L$; and $\mathbf{F}_{body}$, the total body force on the larva due to gravity and buoyancy. $\mathbf{V}_L$ and $\mathbf{\Omega}_L$ are evaluated at a reference point on the larva, X_L (Fig. 2).

The corresponding inertia-less balance for total moments about the reference point on the larva leads to

$$\mathbf{M}_{cilia} + \mathbf{M}_{ext} + \mathbf{M}_{trans}(\mathbf{V}_L) + \mathbf{M}_{rot}(\mathbf{\Omega}_L) + \mathbf{M}_{body} \approx 0 \quad (7)$$

where subscripts have the same interpretations as in (6). This Appendix presents calculations of each of the terms in (6) and (7) for each of the larval geometries considered. These equations can then be used in several ways. For example, they can determine the swimming velocity resulting from a given set of gravity and buoyancy forces, external flow, and ciliary activity. Alternatively, they can determine the gravity and buoyancy forces required to maintain a fixed velocity given the external flow and ciliary activity. By integrating the translational and angular velocities over time, the trajectories followed by freely swimming larvae can be calculated to determine how they interact with external flows. These three applications of the model are the basis of our assessments of larval swimming performance in the discussion below.

Geometry

A larva is considered of fixed geometry (Fig. 2) but variable position. The larva's morphology is defined and its movement within the fluid calculated using two coordinate systems: a fixed global coordinate system (X, Y, Z) and a local coordinate system (x, y, z) whose origin is instantaneously coincident with $\mathbf{X}_L$, a reference point on the larva. The local coordinate system is aligned instantaneously with the larva, whose orientation is specified by the Euler angles (ϕ, θ, ψ) (see, e.g., Hibbeler, 1978). In the following discussion, lower case to refers to quantities in the local coordinate system, and upper case for the global coordinate system.

A position $\mathbf{X}$ in the global coordinates corresponds to the position $\mathbf{x}$ in the local coordinates,

$$\mathbf{x} = \mathbf{R}(\mathbf{X} - \mathbf{X}_L); \quad \mathbf{X} = \mathbf{R}^{-1}\mathbf{x} + \mathbf{X}_L, \quad (8)$$

and the direction vector $\mathbf{e}_X$ in the global coordinates corresponds to $\mathbf{e}_x$ in the local coordinates,

$$\mathbf{e}_x = \mathbf{R}\mathbf{e}_X; \quad \mathbf{e}_X = \mathbf{R}^{-1}\mathbf{e}_x. \quad (9)$$

The rotation matrix for the Euler angles is

$$\mathbf{R} = \begin{pmatrix} -s_\psi c_\theta s_\phi + c_\psi c_\phi & c_\psi s_\phi + s_\psi c_\theta c_\phi & s_\psi s_\theta \\ -s_\psi c_\phi - c_\psi c_\theta s_\phi & c_\psi c_\theta c_\phi - s_\psi s_\phi & c_\psi s_\theta \\ s_\theta s_\phi & -s_\theta c_\phi & c_\theta \end{pmatrix},$$

where $s_\phi = \sin(\phi)$, $c_\phi = \cos(\phi)$, $s_\psi = \sin(\psi)$, $c_\psi = \cos(\psi)$, $s_\theta = \sin(\theta)$, and $c_\theta = \cos(\theta)$.

The larva's external morphology is approximated with a set of n slender cylinders, that are fixed with respect to each other but move as a unit with respect to the global coordinate system. The ith cylinder (for $i = 1, 2, \ldots, n$) is defined by the endpoints of its centerline, $\mathbf{p}_{1_i}$, and $\mathbf{p}_{2_i}$, in local coordinates and its radius, r_i. The instantaneous translational and angular velocities of the larva in the global coordinate system are, respectively,

$$\mathbf{V}_L = \frac{d\mathbf{X}_L}{dt}; \quad \mathbf{\Omega}_L = \begin{pmatrix} s_\psi s_\theta \dot{\phi} + c_\psi \dot{\theta} \\ c_\psi s_\theta \dot{\phi} + s_\psi \dot{\theta} \\ c_\theta \dot{\theta} + \dot{\psi} \end{pmatrix}. \tag{10}$$

The velocity in local coordinates of the ith cylinder's midpoint, $\mathbf{x}_i = (\mathbf{p}_{1_i} + \mathbf{p}_{2_i})/2$, is

$$\mathbf{v}_i = (\omega_L \times \mathbf{x}_i) + \mathbf{v}_L \tag{11}$$

where $\mathbf{v}_L = \mathbf{R}\mathbf{V}_L$ is the translational velocity of the reference point and $\omega_L = \mathbf{R}\mathbf{\Omega}_L$ is the rotational velocity about the reference point of the larva in the local coordinate system.

Inertial components of flow are assumed negligible, so that at any instant the flow is quasi-steady. Slender body theory (see references given in Grünbaum, 1998) is used to relate the force each cylinder exerts on the fluid to the velocity induced around each cylinder. The resulting flow must simultaneously satisfy two conditions: the "no-slip" boundary condition; and the force balance for inertia-less motion. The no-slip boundary condition requires that the velocity of the fluid immediately adjacent to the larva's surface has the same velocity as that surface. For the ith cylinder,

$$\mathbf{u}_i = \mathbf{v}_i, \tag{12}$$

where $\mathbf{u}_i$ is the fluid velocity in local coordinates. Three components contribute to $\mathbf{u}_i$: (*i*) the external flow, if any; (*ii*) the fluid motions induced at the ith cylinder by the forces imparted on the fluid by all the other cylinders; and (*iii*) the effects of active ciliary pumping (see Grünbaum, 1998, for a detailed discussion).

For an arbitrary external flow, $\mathbf{U}_{ext}(\mathbf{X})$, velocity is linearized in the vicinity of the larva in global coordinates as

$$\mathbf{U}_{lin}(\Delta\mathbf{x}) = \hat{\mathbf{U}} + \Delta\mathbf{U}(\Delta\mathbf{X}) \tag{13}$$

where $\hat{\mathbf{U}} = \mathbf{U}_{ext}(\mathbf{X}_L)$ and $\Delta\mathbf{x} = \mathbf{X} - \mathbf{X}_L$ is a small displacement from the reference point on the larva. The linearized velocity deviations in the X, Y, Z directions are

$$\Delta U_1(\Delta \mathbf{X}) := \Delta x_1 \frac{\partial U_{ext1}}{\partial X} + \Delta x_2 \frac{\partial U_{ext1}}{\partial Y} + \Delta x_3 \frac{\partial U_{ext1}}{\partial Z}$$

$$\Delta U_2(\Delta \mathbf{X}) := \Delta x_1 \frac{\partial U_{ext2}}{\partial X} + \Delta x_2 \frac{\partial U_{ext2}}{\partial Y} + \Delta x_3 \frac{\partial U_{ext2}}{\partial Z} \tag{14}$$

$$\Delta U_3(\Delta \mathbf{X}) := \Delta x_1 \frac{\partial U_{ext3}}{\partial X} + \Delta x_2 \frac{\partial U_{ext3}}{\partial Y} + \Delta x_3 \frac{\partial U_{ext3}}{\partial Z}.$$

where all derivatives are evaluated at $\mathbf{X}_L$. Note that because seawater is effectively incompressible in this application, $(\partial U_{ext_1}/\partial X) + (\partial U_{ext_2}/\partial Y) + (\partial U_{ext_3}/\partial Z) = 0$. See Batchelor (1983) for a discussion of how shear, vorticity and pure strain components of an arbitrary flow can be represented in this form.

The fluid velocity in local coordinates at the ith cylinder midpoint is then

$$\mathbf{u}_i = \mathbf{u}_{ext}(\mathbf{x}_i) + \sum_{j=1}^{n} \mathbf{u}_{ind_j}(\mathbf{x}_i) + \sum_{j=1}^{n} \mathbf{u}_{cil_j}(\mathbf{x}_i) \tag{15}$$

where $\mathbf{u}_{ext}(\mathbf{x}_i) = \mathbf{R}(\mathbf{U}_{lin}(\mathbf{R}^{-1}\mathbf{x}_i))$, $\mathbf{u}_{ind_j}(\mathbf{x}_i)$ is the velocity induced at the midpoint of the ith cylinder by the force imparted to the fluid by the jth cylinder, and $\mathbf{u}_{cil_j}(\mathbf{x}_i)$ is the velocity induced at the midpoint of the ith cylinder by the cilia on the jth cylinder. $\mathbf{u}_{ind_j}(\mathbf{x}_i)$ and $\mathbf{u}_{cil_j}(\mathbf{x}_i)$ are functions of cylinder geometries and forces. Expressions for them in terms of Stokeslets and related singularities are found in Grünbaum (1998) and references therein. Determination of the cylinder forces that satisfy the no-slip boundary condition involves inversion of a large linear system, as discussed in Grünbaum (1998).

Force balances

Because $\mathcal{R}e \ll 1$ for the flow around the larva, forces and moments on each part of the larva are proportional to their respective velocity components. The force on the ith cylindrical element by the local fluid velocity, $\hat{\mathbf{u}}_i$, relative to the element are related by

$$\mathbf{f}_i = K_{n_i} L_i \hat{\mathbf{u}}_{n_i} + K_{t_i} L_i \hat{\mathbf{u}}_{t_i}. \tag{16}$$

Here, $\hat{\mathbf{u}}_{t_i}$ is the component of the velocity past the cylinder in the axial direction, and $\hat{\mathbf{u}}_{n_i} = \hat{\mathbf{u}}_i - \hat{\mathbf{u}}_{t_i}$ is the component in the normal (perpendicular) direction. $\hat{\mathbf{u}}_i$ is the flow in which the cylinder is "immersed," i.e., the flow that would exist if that cylinder were removed. K_{n_i} and K_{t_i} are the normal and axial resistance coefficients,

$$K_{n_i} = \frac{8\pi\mu}{2\log(L_i/r_i) + 1}; \quad K_{t_i} = \frac{4\pi\mu}{2\log(L_i/r_i) - 1}. \tag{17}$$

Then,

$$\mathbf{f}_{trans} = \mathbf{K}_{fv}\mathbf{v}_L; \quad \mathbf{K}_{fv} = \begin{pmatrix} k_{fv_{11}} & k_{fv_{12}} & k_{fv_{13}} \\ k_{fv_{21}} & k_{fv_{22}} & k_{fv_{23}} \\ k_{fv_{31}} & k_{fv_{32}} & k_{fv_{33}} \end{pmatrix} \tag{18}$$

$$\mathbf{f}_{rot} = \mathbf{K}_{f\omega}\boldsymbol{\omega}_L; \quad \mathbf{K}_{f\omega} = \begin{pmatrix} k_{f\omega_{11}} & k_{f\omega_{12}} & k_{f\omega_{13}} \\ k_{f\omega_{21}} & k_{f\omega_{22}} & k_{f\omega_{23}} \\ k_{f\omega_{31}} & k_{f\omega_{32}} & k_{f\omega_{33}} \end{pmatrix} \tag{19}$$

where

$$(k_{fv_{i1}} \quad k_{fv_{i2}} \quad k_{fv_{i3}}); \quad (k_{f\omega_{i1}} \quad k_{f\omega_{i2}} \quad k_{f\omega_{i3}}) \tag{20}$$

are the total forces imparted on the larva by a unit translational or angular velocity in the ith direction (in the local coordinate system).

The corresponding equations for moments are

$$\mathbf{m}_{trans} = \mathbf{K}_{mv}\mathbf{v}_L; \quad \mathbf{K}_{mv} = \begin{pmatrix} k_{mv_{11}} & k_{mv_{12}} & k_{mv_{13}} \\ k_{mv_{21}} & k_{mv_{22}} & k_{mv_{23}} \\ k_{mv_{31}} & k_{mv_{32}} & k_{mv_{33}} \end{pmatrix} \tag{21}$$

$$\mathbf{m}_{rot} = \mathbf{K}_{m\omega}\boldsymbol{\omega}_L; \quad \mathbf{K}_{m\omega} = \begin{pmatrix} k_{m\omega_{11}} & k_{m\omega_{12}} & k_{m\omega_{13}} \\ k_{m\omega_{21}} & k_{m\omega_{22}} & k_{m\omega_{23}} \\ k_{m\omega_{31}} & k_{m\omega_{32}} & k_{m\omega_{33}} \end{pmatrix} \tag{22}$$

where

$$(k_{mv_{i1}} \quad k_{mv_{i2}} \quad k_{mv_{i3}}); \quad (k_{m\omega_{i1}} \quad k_{m\omega_{i2}} \quad k_{m\omega_{i3}}) \tag{23}$$

are the total moments imparted on the larva by a unit translational or angular velocity in the ith direction.

The force and moment balances that must be satisfied to give the actual instantaneous translational and angular velocities are given by

$$\mathbf{K}\begin{pmatrix} \mathbf{v}_L \\ \boldsymbol{\omega}_L \end{pmatrix} = -\begin{pmatrix} \mathbf{f}_{cil} \\ \mathbf{m}_{cil} \end{pmatrix} - \begin{pmatrix} \mathbf{f}_{ext} \\ \mathbf{m}_{ext} \end{pmatrix} - \begin{pmatrix} \mathbf{f}_{body} \\ \mathbf{m}_{body} \end{pmatrix} \tag{24}$$

where $\mathbf{K}$ is the block matrix

$$\mathbf{K} = \begin{pmatrix} \mathbf{K}_{f\mathbf{v}} & \mathbf{K}_{f\omega} \\ \mathbf{K}_{m\mathbf{v}} & \mathbf{K}_{m\omega} \end{pmatrix}. \tag{25}$$

The force and moment imparted by the external flow on the larva can be decomposed as in (13), so that

$$\begin{pmatrix} \mathbf{f}_{ext} \\ \mathbf{m}_{ext} \end{pmatrix} = \begin{pmatrix} \mathbf{f}_{const} \\ \mathbf{m}_{const} \end{pmatrix} + \begin{pmatrix} \mathbf{f}_{shear} \\ \mathbf{m}_{shear} \end{pmatrix} \tag{26}$$

in local coordinates. The locally constant component of the flow results in the force and moment

$$\begin{pmatrix} \mathbf{f}_{const} \\ \mathbf{m}_{const} \end{pmatrix} = \begin{pmatrix} \mathbf{K}_{fc} \\ \mathbf{K}_{mc} \end{pmatrix}\hat{\mathbf{u}} \tag{27}$$

where

$$\mathbf{K}_{fc} = \begin{pmatrix} k_{fc11} & k_{fc12} & k_{fc13} \\ k_{fc21} & k_{fc22} & k_{fc23} \\ k_{fc31} & k_{fc32} & k_{fc33} \end{pmatrix}; \quad \mathbf{K}_{mc} = \begin{pmatrix} k_{mc11} & k_{mc12} & k_{mc13} \\ k_{mc21} & k_{mc22} & k_{mc23} \\ k_{mc31} & k_{mc32} & k_{mc33} \end{pmatrix} \tag{28}$$

and $k_{fc_{ij}}$ is the ith component of the total force imparted on the larva by a unit constant external flow in the jth direction, and $k_{mc_{ij}}$ is the ith component of the total or moment imparted on the larva by a unit constant external flow in the jth direction.

The force and moment due to shear are

$$\begin{pmatrix} \mathbf{f}_{shear} \\ \mathbf{m}_{shear} \end{pmatrix} = \mathbf{K}_S \mathbf{S} \tag{29}$$

where

$$\mathbf{S} = \left(\frac{\partial u_1}{\partial x_1}, \frac{\partial u_1}{\partial x_2}, \frac{\partial u_1}{\partial x_3}, \frac{\partial u_2}{\partial x_1}, \frac{\partial u_2}{\partial x_2}, \frac{\partial u_2}{\partial x_3}, \frac{\partial u_3}{\partial x_1}, \frac{\partial u_3}{\partial x_2}, \frac{\partial u_3}{\partial x_3} \right)^T. \tag{30}$$

and the ith row of $\mathbf{K}_S$ is the total force ($i = 1, 2, 3$) or the total moment ($i = 4, 5, 6$) due to unit strengths of the respective velocity components.

Substituting the above expressions into (24), we obtain a system of linear equations defining the quasi-equilibrium force balance,

$$\begin{pmatrix} \mathbf{f}_{cil} \\ \mathbf{m}_{cil} \end{pmatrix} + \mathbf{K} \begin{pmatrix} \mathbf{v}_L \\ \boldsymbol{\omega}_L \end{pmatrix} + \begin{pmatrix} \mathbf{K}_{fc} \\ \mathbf{K}_{mc} \end{pmatrix} \hat{\mathbf{u}} + \mathbf{K}_S \mathbf{S} + \begin{pmatrix} \mathbf{f}_{body} \\ \mathbf{m}_{body} \end{pmatrix} = 0. \tag{31}$$

Several scenarios can now be considered. If the larval motion is known (e.g., to calculate weight capacity, where the larva has no motion) then (31) can be solved for the body forces and moments required to produce the specified velocities:

$$\begin{pmatrix} \mathbf{f}_{body} \\ \mathbf{m}_{body} \end{pmatrix} = -\begin{pmatrix} \mathbf{f}_{cil} \\ \mathbf{m}_{cil} \end{pmatrix} - \mathbf{K} \begin{pmatrix} \mathbf{v}_L \\ \boldsymbol{\omega}_L \end{pmatrix} - \begin{pmatrix} \mathbf{K}_{fc} \\ \mathbf{K}_{mc} \end{pmatrix} \hat{\mathbf{u}} - \mathbf{K}_S \mathbf{S} \tag{32}$$

If the body forces and moments are known but the larva's motion is not, the translational and angular velocities are given by

$$\begin{pmatrix} \mathbf{v}_L \\ \boldsymbol{\omega}_L \end{pmatrix} = -\mathbf{K}^{-1} \left[\begin{pmatrix} \mathbf{f}_{cil} \\ \mathbf{m}_{cil} \end{pmatrix} + \begin{pmatrix} \mathbf{K}_{fc} \\ \mathbf{K}_{mc} \end{pmatrix} \hat{\mathbf{u}} + \mathbf{K}_S \mathbf{S} + \begin{pmatrix} \mathbf{f}_{body} \\ \mathbf{m}_{body} \end{pmatrix} \right] \tag{33}$$

The larva's translation and rotation in global coordinates are $\mathbf{V}_L = \mathbf{R}^{-1}\mathbf{v}_L$ and $\boldsymbol{\Omega}_L = \mathbf{R}^{-1}\boldsymbol{\omega}_L$. For integration of larval trajectories, the rate of change of the Euler angles are then given by

$$\begin{aligned} \dot{\phi} &= \frac{c_\psi}{s_\theta} \omega_{L_2} + \frac{s_\psi}{s_\theta} \omega_{L_1} \\ \dot{\theta} &= c_\psi \omega_{L_1} - s_\psi \omega_{L_2} \end{aligned} \tag{34}$$

$$\dot{\psi} = -\frac{c_\theta c_\psi}{s_\theta}\omega_{L_2} - \frac{c_\theta s_\psi}{s_\theta}\omega_{L_1} + \omega_{L_3}$$

completing the model derivation.

REFERENCES

Batchelor, G. K. 1983. An Introduction to Fluid Mechanics, Cambridge University Press, 635 pp.

Blake, J. R. and A. T. Chwang. 1974. Fundamental singularities of viscous flow. J. Engr. Math., *8,* 23–29.

Boidron-Metairon, I. F. 1988. Morphological plasticity in laboratory-reared echinoplutei of *Dendraster excentricus* (Eschscholtz) and *Lytechinus variegatus* (Lamarck) in response to food conditions. J. Exp. Mar. Biol. Ecol., *119,* 31–41.

Byrne, M. and P. Selvakumaraswamy. 2002. Phylum Echinodermata: Ophiuroidea, *in* Atlas of Marine Invertebrate Larvae, C. M. Young, ed., Academic Press, San Diego, 483–498.

Chwang, A. T. and T. Y. Wu. 1975. Hydromechanics of low-Reynolds-number flow. Part 2. Singularity method for Stokes flows. J. Fluid Mech., *67,* 787–815.

Eckert, G. L. 1998. Larval development, growth and morphology of the sea urchin *Diadema antillarum.* Bull. Mar. Sci., *63,* 443–451.

Eckman, J. E. 1990. A model of passive settlement by planktonic larvae onto bottoms of differing roughness. Limnol. Oceanogr., *35,* 887–901.

Emlet, R. B. 1983. Locomotion, drag, and the rigid skeleton of larval echinoderms. Biol. Bull., *164,* 433–445.

——1991. Functional constraints on the evolution of larval forms of marine invertebrates: experimental and comparative evidence. Am. Zool., *31,* 707–725.

——1994. Body form and patterns of ciliation in nonfeeding larvae of echinoderms: functional solutions to swimming in the plankton? Am. Zool., *34,* 570–585.

Fiksen, O., A. C. W. Utne, D. L. Aksnes, K. Eiane, J. V. Helvik and S. Sundby. 1998. Modelling the influence of light, turbulence and ontogeny on ingestion rates in larval cod and herring. Fish Ocean, *7,* 335–363.

Forward, Jr, R. B. and R. A. Tankersley. 2001. Selective tidal-stream transport of marine animals. Oceangr. Mar. Biol. Ann. Rev., *39,* 305–353.

Franks, P. J. S. 2001. Turbulence avoidance: An alternate explanation of turbulence-enhanced ingestion rates in the field. Limnol. Oceanogr., *46,* 959–963.

Grünbaum, D. 1998. A model of feeding currents in encrusting bryozoans shows interference between zooids within a colony. J. Theor. Biol., *174,* 409–425.

Hancock, G. J. 1953. The self-propulsion of microscopic organisms through liquids. Proc. Roy. Soc. A, *217,* 447–461.

Hart, M. W. 1996. Variation in suspension feeding rates among larvae of some temperate, Eastern Pacific echinoderms. Invert. Biol., *115,* 30–45.

Hart, M. W. and R. R. Strathmann. 1994. Functional consequences of phenotypic plasticity in echinoid larvae. Biol. Bull., *186,* 291–299.

Hendler, G. 1991. Echinodermata: Ophiuroidea, *in* Echinoderms and Lophophorates, Reproduction of Marine Invertebrates, *VI,* A. C. Giese, J. S. Pearse, and V. B. Pearse, eds., Boxwood Press, Pacific Grove, CA, 355–511.

Hibbeler, R. C. 1978. Engineering Mechanics: Dynamics. Macmillan Publishing Co., Inc., 590 pp.

Jiang, H. H., C. Meneveau and T. R. Osborn. 2002a. The flow field around a freely swimming copepod in steady motion. part II: Numerical simulation. J. Plank. Res., *24,* 191–213.

Jiang, H. H., T. R. Osborn and C. Meneveau. 2002b. Chemoreception and the deformation of the active space in freely swimming copepods: a numerical study. J. Plank. Res., *24,* 495–510.

Kelman, D. and R. B. Emlet. 1999. Swimming and buoyancy in ontogenetic stages of the cushion star *Pteraster tesselatus* (Echinodermata: Asteroidea) and their implications for distribution and movement. Biol. Bull., *197,* 309–314.

Lee, H. 1983. Functional differences in feeding and swimming activities correlated with ciliation patterns of pluteus larvae. Am. Zool., *23,* 987.

Lewis, D. M. and T. J. Pedley. 2000. Planktonic contact rates in homogeneous isotropic turbulence: Theoretical predictions and kinematic simulations. J. Theor. Biol., *205,* 377–408.

MacKenzie, B. M. and T. Kiorboe. 2000. Larval fish feeding and turbulence: A case for the downside. Limnol. Oceanogr., *45,* 1–10.

McEdward, L. 1984. Morphometric analysis of the growth and form of an echinopluteus. J. Exp. Mar. Biol. Ecol., *82,* 259–287.

Mladenov, P. V. 1979. Unusual lecithotrophic development of the Caribbean brittle star *Ophiothrix oerstedi*. Mar. Biol., *55,* 55–62.

——1985. Development and metamorphosis of the brittle star *Ophiocoma pumila:* evolutionary and ecological implications. Biol. Bull., *168,* 285–295.

Mogami, Y., J. Ishii and S. A. Baba. 2001. Theoretical and experimental dissection of gravity-dependent mechanical orientation in gravitactic microorganisms. Biol. Bull., *201,* 26–33.

Mortensen, T. 1921. Studies on the development and larval forms of echinoderms. G. E. C. Gad, Copenhagen.

——1927a. Die Echinodermen-Larven. Nordisches Plankton, *5,* 1–30.

——1927b. Handbook of the Echinoderms of the British Isles. Oxford University Press, London.

——1931. Contributions to the study of the development and larval forms of echinoderms. I–II. D. Kgl. Danske Vidensk. Selsk. Skrifter, Naturv. og Math. Series 9, *4,* 1–39.

——1937. Contributions to the study of the development and larval forms of echinoderms. III. D. Kgl. Danske Vidensk. Selsk. Skrifter, Naturv. og Math. Series 9, *7,* 1–65.

——1938. Contributions to the study of the development and larval forms of echinoderms. IV. D. Kgl. Danske Vidensk. Selsk. Skrifter, Naturv. og Math. Series 9, *7,* 1–59.

Müller, J. 1851. Über die Ophiurenlarven des Adriatischen Meeres. Abhandl. Königl. Preuss. Akad. Wiss., Berlin.

Pennington, J. T. and R. B. Emlet. 1986. Ontogenetic and diel vertical migration of a planktonic echinoid larva, *Dendraster excentricus* (Escholtz): occurrence, causes, and probable consequences. J. Exp. Mar. Biol. Ecol., *104,* 69–95.

Pennington, J. T. and R. R. Strathmann. 1990. Consequences of the calcite skeletons of planktonic echinoderm larvae for orientation, swimming, and shape. Biol. Bull., *170,* 121–133.

Pozrikidis, C. 1992. Boundary Integral and Singularity Methods for Linearized Viscous Flow. Cambridge Univ. Press, NY, 271 pp.

Rothschild, B. J. and T. R. Osborn. 1988. Small-scale turbulence and plankton contact rates. J. Plank. Ecol., *10,* 465–474.

Smith, A. B., G. L. J. Patterson and B. Lafay. 1995. Ophiuroid phylogeny and higher taxonomy: morphological and paleontological perspectives. Zool. J. Linn. Soc., *114,* 213–243.

Staver, J. M. and R. R. Strathmann. 2002. Evolution of fast development of planktonic embryos to early swimming. Biol. Bull., *203,* 58–69.

Strathmann, R. R. 1971. The feeding behavior of planktotrophic echinoderm larvae: mechanisms, regulation, and rates of suspension feeding. J. Exp. Mar. Biol. Ecol., *6,* 109–160.

——1975. Larval feeding in echinoderms. Am. Zool., *15,* 717–730.

Strathmann, R. R., L. Fenaux and M. F. Strathmann. 1992. Heterochronic developmental plasticity in larval sea urchins and its implications for evolution of non-feeding larvae. Evolution, *46,* 972–986.

Sundby, S. 1997. Turbulence and ichthyoplankton: Influence on vertical distributions and encounter rates. Scientia Marina, *61,* 159–176.

Thorson, G. 1934. On the reproduction and larval stages of the brittle-stars *Ophiocten sericeum* (Forbes) and *Ophiura robusta* (Ayres) in East Greenland. Medd. Groenland, *100,* 1–21.

Villinski, J. T., J. C. Villinski, M. Byrne, and R. A. Raff. 2002. Convergent maternal provisioning and life-history evolution in echinoderms. Evolution, *65,* 1764–1775.

Visser, A. W., H. Saito, E. Saiz and T. Kiorboe. 2001. Observations of copepod feeding and vertical distribution under natural turbulent conditions in the north sea. Mar. Biol., *135,* 1011–1019.

Wray, G. A. 1995. Evolution of larvae and developmental modes, *in* Ecology of Marine Invertebrate Larvae, L. McEdward, ed., CRC Press, Boca Raton, FL, 413–447.

Yamazaki, H., D. Makas and K. Denman. 2002. Coupling small scale physical processes to biology: towards a Lagrangian approach, *in* The Sea: Biological-Physical Interactions in the Ocean, *12,* A. Robinson, J. McCarthy, and B. Rothschild, eds., John Wiley and Sons, NY, 51–112.

Young, C. M. 1995. Behavior and locomotion during the dispersal phase of larval life, *in* Ecology of Marine Invertebrate Larvae. L. McEdward, ed., CRC Press, Boca Raton, FL, 249–277.

——2002. Atlas of Marine Invertebrate Larvae, Academic Press, San Diego, CA, 630 pp.

Received: *31 March, 2003;* revised: *9 September, 2003.*